

Seminal papers
on
colloidal quantum dots
from
St. Petersburg

Quantum size effect in three-dimensional microscopic semiconductor crystals

A. I. Ekimov and A. A. Onushchenko

S. I. Vavilov State Optics Institute

(Submitted 29 July 1981)

Pis'ma Zh. Eksp. Teor. Fiz. **34**, No. 6, 363–366 (20 September 1981)

The exciton absorption spectrum of microscopic CuCl crystals grown in a transparent dielectric matrix has been studied. The size of the microscopic crystals was varied in a controlled manner from several tens of angstroms to hundreds of angstroms. There is a short-wave shift (of up to 0.1 eV) of the exciton absorption lines, caused by a quantum size effect.

PACS numbers: 61.60. + m, 71.35. + z

Size effects in semiconductors have recently attracted considerable interest. Most of the experiments which have been reported have used quasi-two-dimensional structures grown by molecular epitaxy,¹ MOS structures,² etc. In this letter we report the discovery and a spectroscopic study of a new class of objects that exhibit size effects: three-dimensional microscopic crystals of semiconducting compounds grown in a transparent dielectric matrix.

For the experiments we used multicomponent silicate glasses, with an initial composition including compounds of copper and chlorine at a concentration of the order of 1%. It was found recently³ that when such glasses are heated to a high temperature the characteristic exciton-absorption spectra of CuCl crystals appear in the

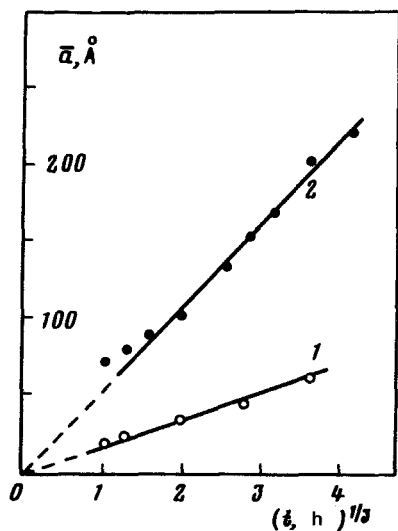


FIG. 1. Dependence of the average radius of the microscopic CuCl crystals on the duration of the heat treatment at the following temperatures: 1—550° C; 2—625° C.

transparency region of the matrix. These spectra directly imply that a microscopically disperse crystalline phase of CuCl forms in the glass as a result of the phase decomposition of a supersaturated solid solution which occurs in the matrix during the heat treatment.

The diffusive phase decomposition of the supersaturated solid solution in the recondensation stage (the stage in which the supersaturation is slight, and the large nucleating regions grow at the expense of the dissolution of small regions) has been studied in detail in a theoretical paper by Lifshitz and Slezov.⁴ They showed that the average radius of the new-phase nuclei, \bar{a} , increases with the time t in accordance with the following asymptotic law during the recondensation growth:

$$\bar{a} = \left(\frac{4\alpha D}{9} t \right)^{1/3}, \quad (1)$$

where D is the diffusion coefficient, and α is a coefficient which is determined by the interfacial surface tension. The concentration of the new phase in the matrix remains constant during the growth. Lifshitz and Slezov also showed that during the recondensation growth of the new phase a steady-state size distribution of the particles is formed. This distribution does not depend on the initial conditions, and its dispersion is relatively small. A analytic expression was derived for this distribution.

Figure 1 shows experimental values of the average radius of the microscopic CuCl crystals precipitated in the matrix by the heat treatment, plotted as a function of the heating time for two different temperatures. The sizes of the microscopic crystals were determined by the method of small-angle x-ray scattering⁵ in the approximation of monodisperse spherical particles.¹⁾ We see from this figure that the experimental data do in fact reveal the behavior $\bar{a} \sim t^{1/3}$, which indicates a recondensation nature of the growth of the microscopic crystals of the semiconducting phase

in the matrix. The slope of the lines in Fig. 1, i.e., the growth rate of the crystals, depends strongly on the heat-treatment temperature and is determined by the diffusion coefficient D , which is an exponential function of the temperature. Accordingly, by choosing the heat-treatment conditions (the temperature and time) appropriately during the growth of semiconducting crystals in a glassy matrix, it is possible to synthesize microscopic crystals of any prespecified size over a broad range, from tens of angstroms to hundreds of angstroms or more. It should also be noted that the particles of the semiconducting phase are in a liquid state during the heat treatment, since the melting point of the CuCl crystals is 440°C , and these crystals are approximately spherical in shape because of the surface tension. It may be that the particles retain this shape during crystallization and that the microscopic CuCl crystals in the matrix can be assumed spherical, in a first approximation.

Figure 2 shows the absorption spectra measured at $T=4.2\text{ K}$ for three samples, differing in the average radius of the microscopic crystals. These spectra were recorded with a dual-beam Perkin-Elmer Model 555 spectrometer with samples $d=0.1\text{ mm}$ in thickness. Such samples could be used because of the relatively low concentration of the crystalline phase in the glass. As can be seen in Fig. 2, at sufficiently large values of the average radius ($\bar{a}=310\text{ \AA}$) the absorption spectrum of the microscopic CuCl crystals dispersed in the matrix has two intense lines ($\lambda=3785\text{ \AA}$ and $\lambda=3865\text{ \AA}$), which result from the excitation of excitons associated with two spin-orbit-split valence subbands. This spectrum is the same as the absorption spectrum of thin CuCl films.⁶ As the average radius of the microscopic crystals is reduced, we observed a significant short-wave shift and a broadening of the exciton-absorption lines remaining in the spectrum, down to the smallest crystal sizes studied, $\bar{a}=20\text{ \AA}$.

The observed dependence of the spectral position of the exciton absorption lines on the microscopic crystals may be a consequence of a quantum size effect.⁷ The current carriers and excitons in a semiconducting crystal in a dielectric matrix are

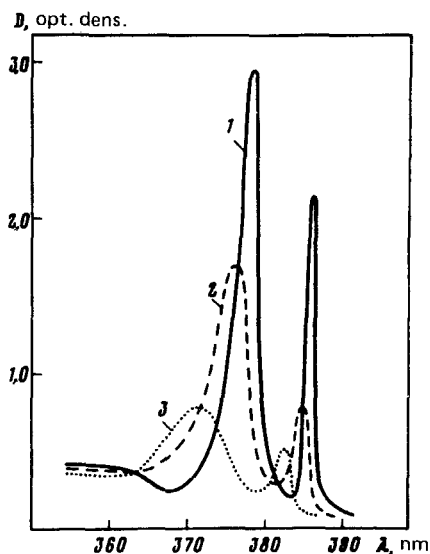


FIG. 2. Absorption spectra at $T=4.2\text{ K}$ of samples having microscopic CuCl crystals with different average radii. 1 - $\bar{a}=310\text{ \AA}$; 2 - $\bar{a}=100\text{ \AA}$; 3 - $\bar{a}=25\text{ \AA}$.

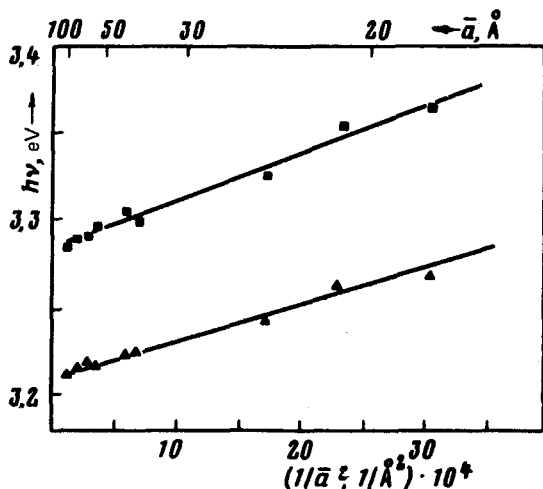


FIG. 3. Dependence of the positions of the exciton absorption lines at $T=4.2$ K on the average radius of the microscopic crystals.

trapped in a potential well whose walls are the boundaries of the microscopic crystal. As the size of the crystal is reduced, the energy of the particles in the potential well increases, and this increase can lead to the observed short-wave shift of the absorption lines. Under the assumption of a spherically symmetric potential well of infinite depth, and if the size dispersion of the particles is neglected, the short-wave shift resulting from the size quantization of a particle of mass m can be described by⁷

$$\Delta E = \hbar^2 \pi^2 / 2 m \bar{a}^2. \quad (2)$$

As can be seen from the experimental dependence of the spectral position of the exciton absorption lines on the average radius of the microscopic crystals (Fig. 3), the short-wave shift is indeed a linear function of $1/\bar{a}^2$ over a broad range of sizes. The effective mass found from the slope of the lines in Fig. 3 and Eq. (2) is $m = 1.2m_0$, where m_0 is the mass of the free electron. This effective mass is at odds with values given in the literature for the effective masses of electrons ($m_e = 0.44m_0$) and holes ($m_h = 3.6m_0$), and it is therefore at odds with the reduced and translational masses of excitons in CuCl crystals.⁸ The discrepancy may be caused primarily by the size dispersion of the particles, which must be taken into account for measuring the radius of the microscopic crystals by the x-ray scattering method and also in determining the effective mass from the dependence of the short-wave shift on $1/\bar{a}^2$.

We wish to thank V. I. Safarov for useful discussions and V. A. Tsekhomskii for furnishing the glass samples.

¹⁾We wish to thank V. V. Golubkov for carrying out the x-ray measurements.

1. R. Dingle, in: *Advances in Solid State Physics*, 1975, XV, 21 P. W.
2. A. Hartstein and A. Fowler, *Proceedings of the Thirteenth International Conference on the Physics of Semiconductors*, Rome, 1976, 741.
3. A. I. Ekimov, A. A. Onushchenko, and V. A. Tsekhomskii, *Fiz. Khim. Stekla* 6, 511 (1980).
4. I. M. Lifshitz and V. V. Slezov, *Zh. Eksp. Teor. Fiz.* 35, 479 (1958) [*Sov. Phys. JETP* 8, 331

(1959)].

5. V. V. Golubkov, A. P. Titov, and E. A. Porai-Koshits, *Prib. Tekh. Eksp.* No. 1, 215 (1975).
6. S. Nikitine, in: *Progress in Semiconductors*, Vol. 6, 1962, p. 269.
7. A. S. Davydov, *Kvantovaya mekhanika*, Moscow, 1963, p. 149. (Quantum Mechanics, Pergamon Press, New York, 1965).
8. N. Kato, T. Goto, T. Fujii, and M. Ueta, *J. Phys. Soc. Jpn.* 36, 169 (1974).

Translated by Dave Parsons

Edited by S. J. Amoretty

Interband absorption of light in a semiconductor sphere

Al. L. Éfros and A. L. Éfros

(Submitted July 27, 1981)

Fiz. Tekh. Poluprovodn. 16, 1209-1214 (July 1982)

A very simple model is used to allow for the influence of size quantization on interband absorption in a semiconductor sphere. Expressions are obtained for the absorption coefficients of light in three limiting cases; when the radius of a semiconductor sphere a is less than the Bohr radii of electrons a_e and holes a_h ; when $a_h \ll a \ll a_e$; finally, when $a_h \ll a$ and $a_e \ll a$. It is shown that in the first two cases the short-wavelength shift of the maximum of the absorption coefficient is proportional to $\hbar^2/m_e a^2$, where m_e is the electron mass. However, if the sphere radius obeys $a \ll a_e$ and $e \ll a_h$, the shift is determined by the total exciton mass $M = m_e + m_h$ and it is proportional to \hbar^2/Ma^2 . The case of a mixture of spheres is considered and the distribution of the radii is described by the Lifshitz-Slezov formula.

PACS numbers: 78.20.Bh, 71.70.Ms, 71.55.Dp, 78.50.Ge

1. Optical properties of systems with an insulating matrix containing semiconductor inclusions have been investigated experimentally in recent years.^{1,2} Such systems are prepared under conditions such that it is possible to regard semiconductor inclusions as spherical particles with a small dispersion of the radii. It is very important to note that it is possible to produce systems in which the average radius of semiconductor particles varies practically continuously. Therefore, a study of the optical properties of such systems as a function of the sphere radius provides a powerful method for determining the parameters of semiconductors and this method is largely analogous to the magneto-optic techniques.

Size quantization of electron and hole states occurs in a semiconductor sphere and the result is that the optical lines shift as a function of the sphere radius. This is in fact observed experimentally.¹ We shall not try to explain completely the results of such experiments. We shall simply propose here a theoretical description of this phenomenon in terms of a very simple model with a standard energy band scheme. It seems to us that such a description is the essential first step in a study of this new range of phenomena.

2. We shall assume that the electron (conduction) and hole (valence) bands are parabolic with the masses m_e and m_h , respectively, where $m_e \ll m_h$. Then, the nature of the size quantization process is governed by the relationship between three lengths: a , a_e , and a_h , where a is the sphere radius, and $a_e = \hbar^2 \kappa / m_e e^2$ and $a_h = \hbar^2 \kappa / m_h e^2$ are the Bohr radii of an electron and a hole, respectively, in the case of a semiconductor whose permittivity is κ (e is the electron charge). The proposed theory is based on the effective mass method, i.e., on the assumption that the important lengths are small compared with the lattice constant. We shall assume that the wave functions of electrons and holes vanish on the surface of a sphere, which corresponds to an infinitely high potential

well surrounding the sphere.

We shall begin with the case of strong size quantization when $a \ll a_h$ and $a \ll a_e$. The separation between the size-quantization levels of electrons and holes is of the order of $\hbar^2/m_e a^2$ and $\hbar^2/m_h a^2$, respectively. These separation energies are large compared with the energy of the Coulomb interaction between an electron and a hole, which is of the order of $e^2/\kappa a$. Therefore, in the first approximation, the Coulomb interaction can be ignored. The wave functions of electrons and holes in a spherically symmetric well with infinitely high walls are

$$\Psi_{n, l, m}(r, \vartheta, \varphi) = Y_{l, m}(\vartheta, \varphi) \frac{\sqrt{2}}{a\sqrt{r}} \frac{J_{l+1/2}(k_{l, n} r)}{J_{l+1/2}(k_{l, n} a)} \quad (1)$$

Here, $Y_{l, m}$ are the normalized spherical functions; l is the momentum; m is the projection of the momentum along a certain direction; J_ν is a Bessel function. The quantities $k_{l, n}$ are given by

$$J_{l+1/2}(k_{l, n} a) = 0 \quad (2)$$

(n is the serial number of the root of the Bessel function for a given value of l). The electron and hole energy levels are

$$E_{l, n}^{e, h} = \frac{\hbar^2 k_{l, n}^2}{2m_{e, h}} \quad (3)$$

It follows from Eq. (2) that the quantity $k_{l, n}$ can be represented in the form

$$k_{l, n} = \frac{\varphi_{l, n}}{a} \quad (4)$$

where $\varphi_{l, n}$ is a universal set of numbers independent of a . In the special case when $l = 0$, we have

$$\varphi_{0, n} = \pi n \quad (n = 1, 2, \dots) \quad (5)$$

If $l \neq 0$, an analytic expression cannot be obtained for

$\psi_{l,n}$. The lowest terms can be found in Ref. 3.

We shall now consider the process of interband absorption of light. From the experimental point of view the most interesting case is the one when the absorption length is large compared with the sphere radius. We shall calculate a quantity K which relates the energy absorbed by a sphere per unit time to the time-average value of the square of the electric field of the incident wave. Multiplication of K by the number of spheres per unit volume gives the electrical conductivity of the system at the field frequency and this conductivity is related in the usual manner to the absorption coefficient of light.

In the case of allowed transitions the quantity K can be represented in the form

$$K = A \sum_{\substack{n, n' \\ l, l' \\ m, m'}} \left| \int \Psi_{n, l, m}^* \Psi_{n', l', m'}^{\hbar} d\tau \right|^2 \delta(\Delta - E_{ln}^e - E_{l'n'}^h). \quad (6)$$

Here, A is proportional to the square of the modulus of the matrix element of the dipole moment calculated using Bloch functions; $\Delta = \hbar\omega - E_g$; ω is the frequency of the incident light; E_g is the band gap of a semiconductor of unbounded size which is subjected to the same conditions (temperature and pressure) as the investigated sphere. The orthogonality of the wave functions of Eq. (1) has the effect that the numbers n and l are conserved in the transitions, whereas the sign of m is reversed:

$$\left| \int \Psi_{n, l, m}^* \Psi_{n', l', m'}^{\hbar} d\tau \right|^2 = \delta_{nn'} \delta_{ll'} \delta_{m, -m'}. \quad (7)$$

Allowing for the degeneracy of m , we obtain

$$K = A \sum_{l, n} (2l+1) \delta\left(\Delta - \frac{\hbar^2}{2\mu} k_{ln}^2\right), \quad (8)$$

where $\mu = m_e m_h / (m_e + m_h)$ is the reduced mass. Therefore, a series of discrete lines should be observed as a result of interband absorption. The absorption threshold is

$$\hbar\omega_{01} = E_g + \frac{\hbar^2 \pi^2}{2\mu a^2}. \quad (9)$$

Hence, we obtain a law according to which the effective band gap increases on reduction in the sphere radius a . The other lines shift toward shorter wavelengths in accordance with the law

$$\hbar\omega_{ln} = E_g + \frac{\hbar^2}{2\mu a^2} \gamma_{ln}^2. \quad (10)$$

If the width of the lines is comparable with the separation between them, size quantization should be manifested by aperiodic oscillations of the absorption with maxima of these oscillations shifting toward shorter wavelengths in accordance with the law $1/a^2$. If $\Delta \gg \hbar^2 \pi^2 / 2\mu a^2$, the oscillatory part becomes small compared with the monotonic component and the latter is described by the classical formula

$$K = A \frac{4\pi}{3} a^3 \frac{\mu^3}{\sqrt{2} \pi^2 \hbar^3} \sqrt{\Delta}. \quad (11)$$

This formula (11) does not allow at all for size quantization and it is easily obtained from Eq. (8) by adopting the

quasiclassical approximation.

3. We shall now consider the case when $a_h \ll a \ll a_e$ and allow for the interaction between an electron and a hole. The energy of electron motion is considerably higher than the energy of a heavy hole, so that the electron potential acting on a hole can be regarded as averaged over the electron motion (adiabatic approximation).

The motion of an electron is described by a wave function of the type given by Eq. (1) so that a hole experiences a spherically symmetric potential

$$V_{n, l, m}(r) = -\frac{e^2}{\alpha} \int \frac{|\Psi_{n, l, m}(r')|^2}{|r-r'|} d^3 r'. \quad (12)$$

The wave functions $\chi_{n, l', m'}$ and the energy levels $E_{n, l', m'}^{h, l'}$ of a hole are found by solving the Schrodinger equation using the potential (12) and the boundary condition, which specifies that the wave functions vanish on the surface of the sphere. In view of the spherical symmetry of the potential, the quantum numbers of the problem are the orbital l' and azimuthal m' numbers, as well as the radial number t . In the adiabatic approximation the wave function of an electron-hole pair is

$$\Psi(r_e, r_h) = \Psi_{n, l, m}(r_e) \chi_{n, l', m'}^{h, l'}. \quad (13)$$

The potential (12) has a minimum at the center of the sphere and it is of the order of $e^2/\mu a$ at its minimum. For the lowest values of l and n , the potential varies over a characteristic distance of the order of a , so that the condition $a_h \ll a$ allows us to expand the potential as a series near the point $r = 0$; we are thus faced with a problem of an isotropic three-dimensional oscillator (see Ref. 3). For simplicity, we shall consider the case when $l = 0$. Then,

$$V_{n, 0, 0}(r) = -\frac{e^2}{\alpha a} \beta_n + \frac{m_h \omega_n^2 r^2}{2}, \quad (14)$$

where

$$\beta_n = 2 \int_0^{\pi} \frac{\sin^2 y}{y} dy, \quad (15)$$

$$\hbar\omega_n = \left[\frac{2}{3} \frac{\hbar^2 \pi^2 n^2}{m_h a^2} \frac{e^2}{\alpha a} \right]^{1/2}. \quad (16)$$

The energy levels of a hole are described by

$$E_{n, 0, 0}^{h, l'} = -\frac{e^2}{\alpha a} \beta_n + \hbar\omega_n \left(2t + l' + \frac{3}{2} \right), \quad (17)$$

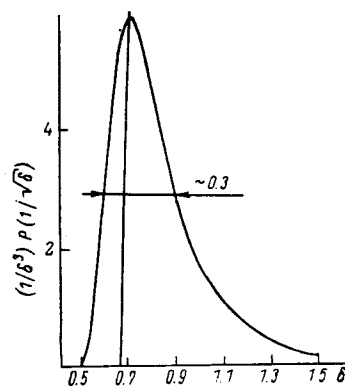


FIG. 1. Dependence of $P(1/\sqrt{\delta})/\delta^3$ on the dimensionless parameter δ .

where $t = 0, 1, 2, \dots$. It is permissible to expand Eq. (14) and to use Eq. (17) if

$$\hbar\omega_n \ll \frac{e^2}{\alpha a}, \quad 2\hbar\omega_n t \ll \frac{e^2}{\alpha a}. \quad (18)$$

For moderately large values of n and t , these inequalities can be satisfied if $a_h \ll a$. In the case of large values of n , when the first of the inequalities in Eq. (18) is no longer obeyed, the Coulomb interaction of a hole and an electron can be regarded as weak, so that in the first approximation the wave function of a hole is described by Eq. (1).

In this case an allowance for the electron-hole interaction has the effect that every line in the interband optical absorption spectrum corresponding to given values of l and n [see Eq. (8)] is converted into a series of closely spaced lines corresponding to different values of the orbital number t . The quantity K is then

$$K = A \sum_{\substack{t \\ l, m, n}} |\Psi(r_e, r_h) \delta(r_e - r_h) dr_e dr_h|^2 \delta(\Delta - E_{ln} - E_{nl}'). \quad (19)$$

Substituting Eq. (13) into Eq. (19), we obtain the selection rules $l = l'$ and $m = -m'$.

We shall now discuss in detail the structure of a transition associated with the lowest electron level corresponding to $l = 0, n = 1$. The function $\chi_{100}^{(0)}$ can be expressed in terms of odd Hermite polynomials (see Ref. 3). When the inequalities (18) are satisfied, this function falls over a distance which is short compared with a . Therefore, we find that

$$\int_0^a \Psi_{100}(r) \chi_{100}^{(0)}(r) r^2 dr = \Psi_{100}(0) \int \chi_{100}^{(0)}(r) r^2 dr. \quad (20)$$

Using Eqs. (19) and (20), and also the explicit form of the functions $\chi_{100}^{(0)}$, we obtain

$$K = A 2\pi^{3/2} \left(\frac{\hbar}{m_e \omega_1}\right)^{3/2} \frac{1}{a^3} \sum_t \frac{(2t+1)!}{2^{2t} (t!)^2} \delta\left(\Delta - \frac{\pi^2 \hbar^2}{2m_e a^2} + \frac{e^2}{\alpha a} \beta_1 - \hbar\omega_1 \left(2t + \frac{3}{2}\right)\right). \quad (21)$$

The most important feature of the above case is that the optical line shift caused by a change in the sphere radius a is described - in the first approximation - by Eq. (10), i.e., it is determined by the size quantization of an electron and, consequently, by the electron mass.

4. We shall now consider the case when $a_h \ll a$ and $a_e \ll a$. The highest energy is now the binding energy F_{ex} of an exciton. If we assume that the center of mass of an exciton is at a fixed point and that this point is located at a distance from the surface of the sphere which is large compared with a_e , the influence of the surface on the exciton binding energy is found to be exponentially weak. We shall not be interested in these exponentially small effects and we shall allow for the shift of an exciton line with changes in the sphere radius, which appears because of the size quantization of the motion of an exciton as a whole. The wave function of an exciton can be represented in the form

$$\Psi(r_e, r_h) = \varphi(r) \Psi_{l, m, n}(R), \quad (22)$$

where $r = r_e - r_h$; $R = (m_e r_e + m_h r_h)/(m_e + m_h)$; $\varphi(r)$

is the wave function of relative motion corresponding to the ground or low excited state. The function $\Psi_{l, m, n}$ is given by Eq. (1) and it describes the motion of the center of mass subject to the boundary conditions on the sphere surface. The exciton energy is

$$E_{l, m, n} = \frac{\hbar^2 k_{ln}^2}{2M} - E_{ex}, \quad (23)$$

where $M = m_e + m_h$. The quantity K is now given by

$$K = A \sum_{l, m, n} |\varphi(0)|^2 \left| \int \Psi_{l, m, n}(R) dR \right|^2 \delta\left(\Delta - E_{ex} - \frac{\hbar^2 k_{ln}^2}{2M}\right), \quad (24)$$

which shows that only the states with $l = m = 0$ contribute to the absorption process. The relative motion should also have an s state. Otherwise, we have $\varphi(0) = 0$. For the ground state we find that $\varphi(0) = (\pi a_{ex}^3)^{-1/2}$, where a_{ex} is the exciton radius (in the hydrogen-like case this radius is close to a_e). In the vicinity of this state, we have

$$K = A \frac{6}{\pi^2} \frac{4\pi}{\pi a_{ex}^3} \frac{1}{3} a^3 \sum_n \frac{1}{n^2} \delta\left(\Delta + E_{ex} - \frac{\hbar^2 \pi^2 n^2}{2M a^2}\right). \quad (25)$$

The most important feature of this case is that the shift of an exciton level as a result of a change in the sphere radius is governed by the total mass of an exciton. The maximum oscillator strength is exhibited by the transitions with $n = 1$. In this case we have

$$\Delta = -E_{ex} + \frac{\hbar^2 \pi^2}{2M a^2}. \quad (26)$$

5. Up to now we have considered the absorption of a system consisting of semiconductor spheres of the same size. In a comparison with the experimental results the quantity K given by Eqs. (8), (11), (21), and (25) may be multiplied by the concentration of the spheres. We shall allow for the dispersion of the sphere radii, which appears in systems investigated in Refs. 1 and 2.

An analysis made in Refs. 1 and 2 allows us to postulate that the formation of single-crystal semiconductor inclusions (particles) in these experiments is primarily due to recondensation processes. Such a process was considered theoretically in detail by Lifshitz and Slezov,⁴ who obtained the distribution function $P(u)$ of the radii of spheres formed in this way:

$$P(u) = \frac{3^* u^2 \exp[-1/(1-2u/3)]}{2^{3/2} (u+3)^{3/2} (3/2-u)^{1/2}}, \quad u < 3/2, \quad (27)$$

$$P(u) = 0 \quad u > 3/2.$$

The probability of finding a sphere with a radius a within an interval da is $P(a/\bar{a}) da/\bar{a}$, where \bar{a} is the average size of a sphere.

The function $P(u)$ is normalized and it has the following properties:

$$\int_0^{3/2} P(u) du = \int_0^{3/2} P(u) u du = 1. \quad (28)$$

We shall consider the situation when $a \gg a_e$ and $a \gg a_h$. In this case an allowance for the dispersion changes Eq.

(25) for K to

$$K = A \frac{6}{\pi^2} \frac{1}{\pi a_{ex}^3} \frac{4}{3} \pi \bar{a}^3 \sum_n \frac{1}{n^2} \int_0^{3/2} du u^2 P(u) \delta \left(\Delta + E_{ex} - \frac{\hbar^2 \pi^2 n^2}{2M\bar{a}^2 u^2} \right). \quad (29)$$

Introducing a dimensionless variable $\delta = (\Delta + E_{ex}) / (\hbar^2 \pi^2 / 2M \bar{a}^2)^{-1}$, we find that integration yields

$$K = A \frac{6}{\pi^2} \frac{1}{\pi a_{ex}^3} \frac{4}{3} \pi \bar{a}^3 \left(\frac{\hbar^2 \pi^2}{2M\bar{a}^2} \right)^{-1} \sum_n \frac{1}{n^2} \left(\frac{n}{\sqrt{\delta}} \right)^6 P \left(\frac{n}{\sqrt{\delta}} \right). \quad (30)$$

It follows that an allowance for the dispersion gives rise to a series of broad maxima of the absorption coefficient, with the profiles and positions given by the functions $(n^6/\delta^3) P(n/\sqrt{\delta})$. Figure 1 shows the explicit form of this function for the lowest transition ($n = 1$) characterized by the maximum oscillator strength. The maximum of this curve corresponds to $\delta = 0.67$. Hence, it follows that the shift of an exciton line associated with a transition to the ground state with $n = 1$ obeys the law

$$\Delta \approx -E_{ex} + 0.67 \frac{\hbar^2 \pi^2}{2M\bar{a}^2}. \quad (31)$$

A comparison of Eqs. (26) and (31) shows that the use of Eq. (26) in an analysis of the experimental results will overestimate the value of M because no allowance is made for the dispersion.

Figure 1 can be used also to find the width of the maximum associated with the dispersion. This width is $\approx 0.3(\hbar^2 \pi^2 / 2M\bar{a}^2)$ and it increases on reduction in the average sphere radius a as $1/\bar{a}^2$.

If $\bar{a} \ll a_e$ and $\bar{a} \ll a_h$, an allowance for the dispersion of the sphere radii characterized by the distribution function (27) modifies the expression for the absorption threshold (9) to

$$\hbar\omega_{01} = E_g + 0.71 \frac{\hbar^2 \pi^2}{2\mu\bar{a}^2}. \quad (32)$$

The theoretical results obtained above are compared with the experimental data in Ref. 5 (following paper).

The authors are grateful to A. I. Ekimov who suggested this investigation.

¹A. I. Ekimov, A. A. Onushchenko, and V. A. Tsekhomskii, *Fiz. Khim. Stekla* **6**, 511 (1980).

²V. V. Golubkov, A. I. Ekimov, A. A. Onushchenko, and V. A. Tsekhomskii, *Fiz. Khim. Stekla* **7**, 397 (1981).

³S. Flugge, *Practical Quantum Mechanics*, Vol. 1, Springer Verlag, Berlin (1971).

⁴I. M. Lifshits and V. V. Slezov, *Zh. Eksp. Teor. Fiz.* **35**, 479 (1958) [*Sov. Phys. JETP* **8**, 331 (1959)].

⁵A. I. Ekimov and A. A. Onushchenko, *Fiz. Tekh. Poluprovodn.* **16**, 1215 (1982).

Translated by A. Tybulewicz

Quantum size effect in the optical spectra of semiconductor microcrystals

A. I. Ekimov and A. A. Onushchenko

(Submitted July 27, 1981)

Fiz. Tekh. Poluprovodn. **16**, 1215-1219 (July 1982)

A study was made of the optical absorption spectra of CuCl microcrystals dispersed in a transparent insulating matrix made of a multicomponent silicate glass. These microcrystals grew in the matrix by diffusive phase precipitation of a super-saturated solid solution during the recondensation stage. The size of microcrystals was increased deliberately during growth from tens to hundreds of ångströms. A strong (up to 0.1 eV) short-wavelength shift was exhibited by the exciton absorption lines on reduction in the microcrystal size and this was due to the quantum size effect.

PACS numbers: 71.35. + z, 78.40.Fy

Various size effects in semiconductors are attracting considerable interest. For example, the development of the molecular epitaxy method, which can be used to grow semiconductor films of thickness down to several lattice constants, has stimulated investigations of the quantum size effect in quasi-two-dimensional structures.¹ Optical spectroscopy methods play an important role in studies of the size effects in semiconductors.

Three-dimensional microcrystals of semiconductor compounds can be grown in a transparent insulating matrix consisting of silicate glass² and their formation can be detected directly from the optical absorption spectra. It is found that the average size of microcrystals in such a matrix can be altered in a deliberate manner during

growth within a wide range from tens to hundreds or more ångströms.³ Such heterogeneous glasses represent a new

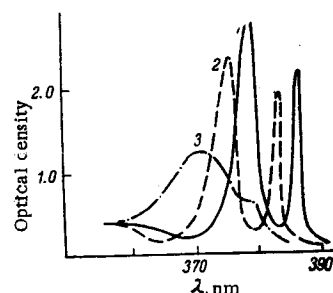


FIG. 1. Absorption spectra of CuCl microcrystals of $\bar{a} = 310$ Å radius recorded at different temperatures T (°K): 1) 4.2; 2) 77; 3) 300.

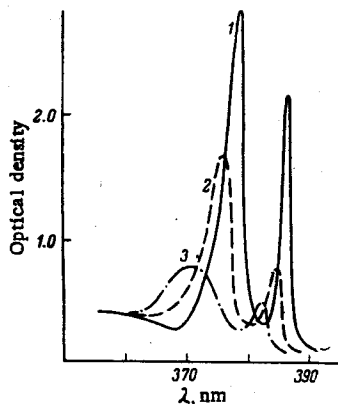


FIG. 2. Absorption spectra of CuCl microcrystals of different average radius obtained at $T = 4.2^\circ\text{K}$. Radius \bar{a} (Å): 1) 310; 2) 100; 3) 25.

and very convenient object for investigating the size effects in semiconductors.

The present paper reports an experimental study of the exciton absorption spectra of CuCl microcrystals dispersed in a transparent insulating matrix. A considerable spectral shift of the exciton absorption lines was observed and this shift was governed only by the microcrystal size. The results obtained were interpreted on the basis of a theory of interband absorption of light by three-dimensional microcrystals⁴ of size comparable with the Bohr radii of carriers.

EXPERIMENTAL METHOD

We investigated silicate glasses containing copper and chlorine compounds in amounts of the order of a few percent. Since the concentrations of copper and chlorine were higher than their solubility limit in the matrix, a system of this kind was a supersaturated solid solution. High-temperature heating of the glasses resulted in a phase decomposition (precipitation) of the supersaturated solid solution and in fluctuation-type formation of nuclei of a new phase. The critical size of the nuclei was governed by the temperature of the heat treatment and by the degree of supersaturation of the solid solution.⁵ The recently observed optical manifestations of the semiconductor phase²—in the form of characteristic exciton absorption spectra, which appeared in the transparency range of the matrix after heating to high temperatures—demonstrated unambiguously the formation of CuCl microcrystals in the glassy matrix as a result of the processes described below.

The subsequent growth of the nuclei of the new phase by diffusive precipitation of the supersaturated solid solution at the recondensation stage, i.e., when the supersaturation was low and the growth of large particles occurred as a result of dissolution of the smaller ones, was considered in detail theoretically in Ref. 6. It was shown there that the increase in the average radius of the nuclei of a new phase considered as a function of the heat treatment duration is given by

$$\bar{a} = \left(\frac{4\alpha D}{9} t \right)^{1/2}, \quad (1)$$

where \bar{a} is the average radius of the nuclei, D is the diffusion coefficient, and α is a coefficient related to the interphase surface tension.

As shown in our earlier investigation,³ the conditions

necessary for the recondensation growth of CuCl microcrystals were satisfied in the range of heat-treatment temperatures $550\text{--}700^\circ\text{C}$, and the average radius of microcrystals did indeed rise linearly as a function of the cubic root of the heat treatment duration, in accordance with Eq. (1). Therefore, variation of the heat treatment conditions (temperature and duration) made it possible to obtain microcrystals of any (previously specified) size ranging from tens to hundreds of ångströms. One should also point out that since the heat treatment temperatures exceeded the melting point of CuCl crystals, equal to 440°C , during growth the nuclei were in the liquid state and because of the surface tension they assumed a nearly spherical shape. Therefore, if the shape of the nuclei was retained during crystallization, the CuCl microcrystals dispersed in the glassy matrix could be regarded, in the first approximation, as spherically symmetric.

Synthesis of semiconductor compounds in an insulating matrix not only provides an important technique for preparing crystals of microscopic size, but also has another important advantage. Since the concentration of the crystalline phase in the glassy matrix is relatively low, it is possible to record directly the absorption spectra of crystals for relatively thick samples prepared by mechanical polishing. In our investigation the absorption spectra of CuCl crystals with an absorption coefficient of 10^5 cm^{-1} at the exciton line maxima were recorded using samples 0.1 mm thick. Measurements were carried out using a Perkin-Elmer Model 555 two-beam automatic spectrophotometer and an Oxford Instruments continuous-flow cryostat; the spectra were recorded at temperatures $T = 4.2\text{--}300^\circ\text{K}$. In all cases the size of CuCl microcrystals was determined earlier³ by the method of small-angle x-ray scattering on the assumption that these microcrystals were spherical monodisperse particles.

EXPERIMENTAL RESULTS

Figure 1 shows the absorption spectra of a sample containing CuCl microcrystals of average size $\bar{a} = 310\text{ Å}$. The spectra were measured at temperatures of 4.2°K (curve 1), 77°K (curve 2), and 300°K (curve 3). It was found that the low-temperature spectra had two strong lines due to the excitation to the ground state of excitons bound to two valence subbands split by the spin-orbit interaction. When temperature was increased, a shift of the exciton absorption lines toward shorter wavelengths

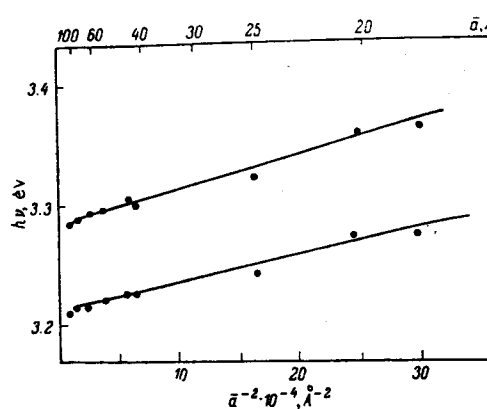


FIG. 3. Dependences of the spectral positions of the exciton absorption lines at $T = 4.2^\circ\text{K}$ on the average radius of microcrystals.

was observed and it was typical of CuCl crystals. The spectral positions of the exciton absorption lines were the same as the values reported in Ref. 7 for thin CuCl films. This indicated that the microcrystals were not compressed hydrostatically by the matrix (in principle, such a compression could result from the difference between the thermal expansion coefficients). The thermal expansion coefficient of CuCl crystals was greater than that of the matrix and, consequently, cooling resulted in faster compression of the microcrystals than of the matrix. Consequently, there should be no hydrostatic compression effects which could shift the exciton absorption lines.

Our investigation demonstrated that the form of the absorption spectra of CuCl microcrystals dispersed in the glassy matrix depended strongly on the microcrystal size and this was true at all temperatures. At $T = 4.2^\circ\text{K}$ we determined the absorption spectra of three samples (Fig. 2) which differed in respect of the microcrystal size. We found that reduction in the microcrystal size resulted in a considerable shift of the exciton absorption lines toward shorter wavelengths and this was accompanied by broadening of these lines. The shift was different for the two lines so that the energy separation between them increased from $\Delta = 70$ to $\Delta = 100$ meV. It was interesting to note that the exciton absorption lines were observed in the spectrum even for the smallest microcrystals studied in the present case ($\bar{a} = 18 \text{ \AA}$), when the total number of atoms in a microcrystal was just a few hundred. Similar dependences of the spectral positions of the exciton absorption lines on the average radius of microcrystals in a sample were observed also at 77 and 300°K .

The effects observed could be attributed to the influence of the quantum size effect⁸ on the band and exciton states in the investigated microcrystals. In fact, carriers and excitons in a microcrystal surrounded by an insulating matrix are known to be localized in a three-dimensional potential well with boundaries at the crystal surface. Reduction in the size of the potential well increases the minimum energy of the particles localized in it and this is manifested by an effective increase in the band gap on reduction in the microcrystal size.

DISCUSSION OF THE RESULTS

The influence of the size quantization effect on the exciton and interband absorption spectra of spherical semiconductor microcrystals is considered in Ref. 4 for the case of a potential well of infinite depth. The binding energy and radius of excitons in CuCl crystals are $E_{\text{ex}} = 0.2$ eV and $r_{\text{ex}} = 7 \text{ \AA}$, respectively.⁷ Therefore, the Bohr radii of carriers and excitons are much smaller than the average radius of microcrystals. As shown in Ref. 4, in the case of monodisperse (constant-size) microcrystals, the spectral positions of the exciton absorption lines are given by

$$\hbar\nu = E_g - E_{\text{ex}} + \frac{\hbar^2\pi^2}{2M\bar{a}^2}, \quad (2)$$

where E_g is the band gap of the crystal, E_{ex} is the exciton binding energy, and M is the translation mass of excitons. It is clear from the above formula that if we

ignore the influence of the microcrystal size on the exciton binding energy, we find that the quantum size effect results in a linear dependence on $1/\bar{a}^2$ of the short-wavelength shift of the exciton absorption lines. The slope of the dependence of the shift on $1/\bar{a}^2$ is governed solely by the translational mass of excitons.

Figure 3 gives the experimental dependences of the spectral positions of the exciton absorption lines on the average radius of microcrystals. It is clear from this figure that in a wide range of microcrystal sizes the short-wavelength shift of the exciton absorption lines does indeed vary linearly with $1/\bar{a}^2$. The translational mass of excitons determined from the slope of the straight lines in Fig. 3 is $M = 1.3m_0$ for the excitons bound to the upper valence subband and $M = 1.2m_0$ for those bound to the lower valence subband (m_0 is the mass of a free electron).

As shown in Ref. 4, the slope of the experimental curves and, consequently, the effective mass may be influenced considerably by the dispersion of the particle size. It is demonstrated in Ref. 6 that recondensation growth of nuclei establishes a steady-state distribution of the particle size independent of the initial conditions; an analytic expression is obtained for this distribution in Ref. 6. The profile of the exciton absorption lines is calculated in Ref. 4 allowing for the particle size distribution obtained in Ref. 6, and an estimate is made of the influence of this distribution on the slope of the dependence of the short-wavelength shift on $1/\bar{a}^2$. If allowance is made for the dispersion of the particle size, it follows from the results of Ref. 4 that the translational masses of excitons bound to the upper and lower valence subbands are $M = 0.9m_0$ and $M = 0.8m_0$ respectively.

It is reported in the literature that the effective mass of electrons in CuCl crystals is $m_e = 0.44m_0$ and that of holes in the upper valence band is $m_h = 3.6m_0$ (Refs. 7 and 9). We can see that our translational mass $M = m_e + m_h$ differs considerably from the published data. This is primarily due to the fact that the real distribution of the microcrystal size differs greatly from the distribution used in calculations in Ref. 4. In fact, the observed profile of the exciton absorption lines (although clearly asymmetric) is characterized by a much greater half-width than predicted in Ref. 4. If the real particle size distribution is characterized by a much greater dispersion than in Ref. 6, this affects the results of measurements of the microcrystal radii by the small-angle x-ray scattering method and the determination of the effective mass from the shift of the absorption lines.

We can thus see that the problem of determination of the effective mass of carriers in semiconductors by the size quantization method requires a further detailed study.

The authors are grateful to Al. L. Éfros and A. L. Éfros for valuable discussions and to V. A. Tsekhomskii for supplying the samples of glasses containing copper and chlorine.

¹R. Dingle, *Festkörperprobleme* 15, 21 (1975).

²A. I. Ekimov, A. A. Onushchenko, and V. A. Tsekhomskii, *Fiz. Khim. Stekla* 6, 511 (1980).

³V. V. Golubkov, A. I. Ekimov, A. A. Onushchenko, and V. A. Tsekhomskii, *Fiz. Khim. Stekla* 7, 397 (1981).

⁴A. L. Éfros and A. L. Éfros, *Fiz. Tekh. Poluprovodn.* 16, 1209 (1982).

⁵E. M. Lifshitz and L. P. Pitaevskii, *Physical Kinetics*, Pergamon Press, Oxford (1981).

⁶I. M. Lifshitz and V. V. Slezov, *Zh. Eksp. Teor. Fiz.* 35, 479 (1958) [*Sov. Phys. JETP* 8, 331 (1959)].

⁷S. Nikitine, *Progr. Semicond.* 6, 269 (1962).

⁸A. S. Davydov, *Quantum Mechanics*, Pergamon Press, Oxford (1965).

⁹Y. Kato, T. Goto, T. Fujii, and M. Ueta, *J. Phys. Soc. Jpn.* 36, 169 (1974).

Translated by A. Tybulewicz

Size quantization of the electron energy spectrum in a microscopic semiconductor crystal

A. I. Ekimov and A. A. Onushchenko

(Submitted 10 September 1984)

Pis'ma Zh. Eksp. Teor. Fiz. **40**, No. 8, 337–340 (25 October 1984)

The interband absorption spectrum of microscopic CdS crystals ranging in size from ~ 30 to 800 \AA and dispersed in a transparent insulating matrix has been studied. There is a significant ($\sim 0.8\text{-eV}$) shift of the fundamental absorption edge in the short-wavelength direction, and there are oscillations in the interband absorption spectrum caused by quantum size effect.

Golubkov *et al.*¹ have found that microscopic crystals of semiconductor compounds can be grown during the diffusive phase decomposition of a supersaturated solid solution in a transparent insulating matrix. The size of the microscopic crystals

can be varied in a controlled way over a broad range from tens to thousands of angstroms. Such heterophase systems can be combined with the methods of optical spectroscopy to study a variety of effects caused by size quantization of the energy spectrum of quasiparticles in microscopic semiconductor crystals. In particular, we have observed² a size quantization of excitons in microscopic CuCl crystals with dimensions considerably larger than the exciton radius ($a_{\text{exc}} \approx 8 \text{ \AA}$) in this material. In the present letter we report experiments on CdS microscopic crystals ($a_{\text{exc}} \approx 30 \text{ \AA}$) in the other limiting case, in which the exciton radius is greater than the radius of the semiconductor particle. We have observed a size quantization of the energy spectrum of free electrons, and we have determined their effective mass.

The microscopic CdS crystals were grown in the interior of a silicate glass matrix produced from a material to which cadmium sulfide had been added. The crystals were nucleated and grew as the glass samples were heated at a high temperature. The size of the particles and the concentration of the semiconductor phase in each sample were determined by small-angle x-ray scattering in the approximation of monodispersed spherical particles.¹ It was found³ that the dependence of the size of the microscopic crystals on the time and temperature of the heat treatment can be described well by a recondensation mechanism of a diffusive phase decomposition of a supersaturated solid solution that was studied by Lifshitz and Slezov.⁴ In the course of the recondensation, the large particles grow by virtue of the dissolution of finer particles, and the concentration of the precipitated phase remains constant, as does the size distribution of the particles. In this manner we produced a set of samples in which the average radius on the microscopic CdS crystals ranged from $\bar{a} \approx 15 \text{ \AA}$ to $\bar{a} \approx 400 \text{ \AA}$.

In the absorption spectra of samples containing rather large crystals ($\bar{a} \approx 250 \text{ \AA}$), we observe three absorption lines at $T = 4.2 \text{ K}$, which are caused by the excitation of excitons associated with three valence subbands in the hexagonal cadmium sulfide crystals. The parameters of the spin-orbit and crystal splitting of the valence band

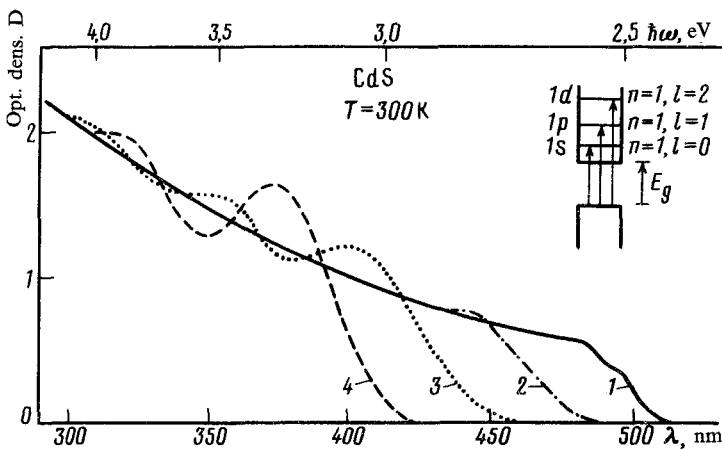


FIG. 1. Absorption spectra of samples containing microscopic CdS crystals of various radii. 1— $\bar{a} = 380 \text{ \AA}$; 2— $\bar{a} = 32 \text{ \AA}$; 3— $\bar{a} = 19 \text{ \AA}$; 4— 14 \AA .

agree well with data in the literature for bulk single crystals.⁵ The microscopic CdS crystals grown in the interior of the glassy matrix are thus of rather high quality from the standpoint of optical spectroscopy.

Figure 1 shows the results of room-temperature measurements of the absorption spectra of four samples, differing in the average radius of the microscopic crystals. For the large crystals we observe the usual interband absorption spectrum, on whose long-wavelength edge there is some structure due to the spin-orbit splitting of the valence band. As the crystal size decreases, there is a shift of the absorption edge in the short-wavelength direction, and oscillations appear in the interband absorption spectrum at a position that also depends on the size of the microscopic crystals. The effective increase in the width of the band gap in the CdS crystals reaches ~ 0.8 eV in the case of the smallest crystals.

The observed effects are evidently due to a quantum size effect. A microscopic semiconductor crystal in an insulating matrix is a three-dimensional potential well that limits the motion of free current carriers, leading to a size quantization of the carrier energy spectrum. The size quantization of electrons and holes in semiconductors was analyzed in the effective-mass approximation by Éfros and Éfros⁶ for spherical microscopic crystals. The case analyzed by them corresponds to the case discussed in Ref. 6, with $a_h < \bar{a} < a_e$, where $a_e = \hbar^2 \kappa / m_e e^2$ and $a_h = \hbar^2 \kappa / m_h e^2$ are the Bohr radii of the electron and the hole. Ignoring the Coulomb interaction, we can describe the position of the absorption lines due to interband transitions to quantum sublevels of the conduction band as a function of the size of the microscopic crystals by the following expression⁶:

$$\hbar\omega_{ln} = E_g + \frac{\hbar^2}{2m_e \bar{a}^2} \varphi_{ln} \quad (1)$$

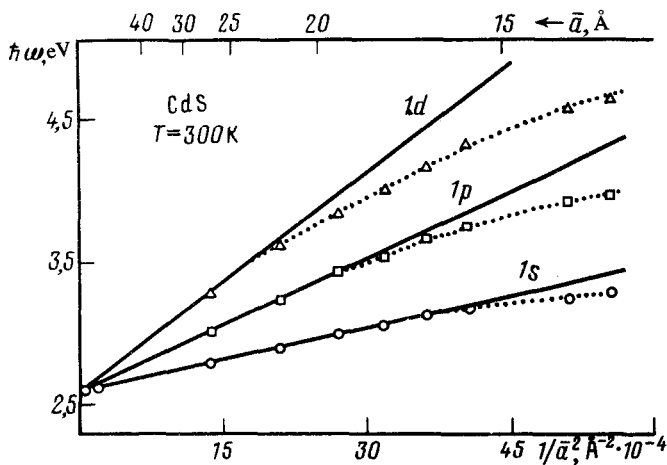


FIG. 2. Position of the absorption edge and of the oscillation maxima versus the radius of the microscopic crystals.

where m_e is the effective mass of the electrons, and φ_{ln} are the roots of the Bessel function ($\varphi_{01} = 3.14$, $\varphi_{11} = 4.49$, $\varphi_{21} = 5.76$).⁷ The quantization of the energy spectrum of the electrons in the conduction band thus gives rise to a short-wavelength shift of the edge and to the appearance of oscillations in the interband absorption spectrum. Figure 1 shows the energy diagram of the optical transitions. It can be seen from the expression above that the short-wavelength shift of the absorption edge and of the oscillations is described by a linear dependence on $1/\bar{a}^2$, and the only parameter that determines the slope of this dependence is the effective electron mass of the material under study.

The points in Fig. 2 are the experimental positions of the absorption edge and the oscillation maxima, plotted against the radius of the microscopic crystals. For large radii the absorption edge of the microscopic crystals coincides with the absorption edge of bulk single crystals.⁵ The straight lines are drawn from (1) with $m_e = 0.21m_0$. We see that over a broad range of the radius of the microscopic crystals there is a good agreement between the experimental points and the theory. The effective electron mass determined in this manner agrees well with the value found for bulk CdS single crystals⁵ ($m_e = 0.205m_0$).

There are several reasons for the deviation of the experimental points from the theoretical predictions at small radii of the microscopic crystals. First, the assumption in the theory that the potential well is infinitely deep is not unshiftable at these large short-wavelength shifts of the size-quantization levels of the electrons ($\sim 1-2$ eV). Second, the conduction band may be nonparabolic at these electron energies. Both of these factors could cause a deviation of the experimental points from linearity, and the deviation would increase with the level energy, as is observed experimentally. Furthermore, an analysis of the experimental results must allow for the Coulomb interaction between the electron and the hole, which depends on both the size of the microscopic crystal and the dielectric constant of the matrix.⁸

We wish to thank Al. L. Éfros for useful discussions of these results.

¹V. V. Golubkov, A. I. Ekimov, A. A. Onushchenko, and A. V. Tsekhomskii, *Fiz. Khim. Stekla* **6**, 511 (1980).

²A. I. Ekimov and A. A. Onushchenko, *Pis'ma Zh. Eksp. Teor. Fiz.* **34**, 363 (1981) [*JETP Lett.* **34**, 345 (1981)].

³A. I. Ekimov and A. A. Onushchenko, *Tr. Vses. konf. po fiz. polupr.* (Proceedings of the All-Union Conference on Semiconductor Physics), Baku, Vol. 2, 1982, p. 176.

⁴I. M. Lifshitz, and V. V. Slezov, *Zh. Eksp. Teor. Fiz.* **35**, 479 (1958) *Sov. Phys. JETP* **8**, 331 (1959)].

⁵*Physics and Chemistry of II-VI Compounds* (Russ. transl. Mir, Moscow, Ch. 7).

⁶Al. L. Éfros and A. L. Éfros, *Fiz. Tekh. Poluprovodn.* **16**, 1209 (1982) [*Sov. Phys. Semicond.* **16**, 772 (1982)].

⁷A. S. Davydov, *Kvantovaya mekhanika*, FM, 1693, p. 149 (Quantum Mechanics, Pergamon, New York, 1965).

⁸L. V. Keldysh, *Pis'ma Zh. Eksp. Teor. Fiz.* **29**, 716 (1979) [*JETP Lett.* **29**, 658 (1979)].

Translated by Dave Parsons

Edited by S. J. Amoretti

Size quantization of excitons and determination of the parameters of their energy spectrum in CuCl

A. I. Ekimov, A. A. Onushchenko, A. G. Plyukhin, and A. L. Éfros

A. F. Ioffe Physicotechnical Institute, Academy of Sciences of the USSR, Leningrad

(Submitted 8 November 1984)

Zh. Eksp. Teor. Fiz. **88**, 1490–1501 (April 1985)

Optical spectroscopy methods were used to investigate the size quantization of the energy spectrum of excitons in CuCl microcrystals dispersed in a transparent dielectric matrix. The size of microcrystals grown by diffusion-type precipitation of a new phase in a supersaturated solid solution was deliberately varied from tens to thousands of angstroms. It was found that the profile of a luminescence line of free excitons was due to the dispersion of the size of microcrystals described by the Lifshitz–Slezov distribution for the recondensation stage of the growth of microcrystals. A theory of the size quantization of excitons allowing for the complex structure of the valence band was developed. A comparison with the experimental results yielded the energy band parameters describing the energy spectrum of excitons in a CuCl crystal.

I. INTRODUCTION

It has been recently demonstrated that ultradisperse semiconducting microcrystals can be grown inside a transparent dielectric matrix.¹ A method for the growth of microcrystals by a diffusion-type precipitation of a new phase of a supersaturated solid solution developed by Golubkov *et al.*¹ makes it possible to control the size of the resultant particles over a wide range from tens to thousands of angstroms. The silicate glass matrix is transparent in a wide range of wavelengths from ultraviolet to the near infrared part of the spectrum, so that it is possible to use optical spectroscopy methods for investigating the properties of microcrystals.

Heterophase systems of this kind represent a new class of objects for investigating various “size” effects in semiconductors and, in particular, the quantum size effect. In fact, a semiconducting microcrystal in a dielectric matrix represents a three-dimensional potential well of size which limits the region of motion of quasiparticles. Consequently, free motion of quasiparticles in a microcrystal is possible only for certain values of the energy and the energy spectrum in quantized.^{2–4}

The problem of manifestation of the size quantization effect in the exciton and interband absorption spectra of spherical semiconducting microcrystals is considered theoretically in Ref. 5. It is shown that the influence of the quantum size effect on the absorption and luminescence spectra of microcrystals depends strongly on the ratio of the exciton radius a_{ex} to the microcrystal radius a . In the case when $a_{ex} \ll a$, an exciton is quantized as a whole and the influence of the boundaries of a microcrystal on the exciton binding energy is exponentially small. In the other limiting case, when $a_{ex} \gg a$, we can ignore the Coulomb interaction between electrons and holes. In the interband absorption case we should observe aperiodic oscillations associated with transitions between the size quantization levels of holes and electrons.

The exciton size quantization effect was reported for CuCl microcrystals in Ref. 2 and preliminary results of an investigation of the effect were published in Ref. 3. The other

limiting case of $a_{ex} \gg a$ was also studied using CdS microcrystals, which exhibited oscillations in the interband absorption spectrum due to the size quantization of the energy spectrum of free electrons.⁴

In the case when $a_{ex} \ll a$ the position of the exciton line maximum considered as a function of the average radius of microcrystals \bar{a} is described by the following expression⁵:

$$\hbar\omega = E_g - E_{ex} + \hbar^2 \pi^2 K / 2M\bar{a}^2, \quad (1)$$

where E_g is the band gap; E_{ex} is the binding energy of an exciton; M is the translational mass of an exciton; K is a numerical coefficient governed by the size distribution of microcrystals. However, the model of a simple exciton energy band with a parabolic dispersion law considered in Ref. 5 does not describe the real band structure of CuCl crystals and gives only the first approximation to the experimental situation.

We shall report a detailed investigation of the dependences of the position and profile of the exciton luminescence and absorption lines of CuCl microcrystals on their size. We shall show that the shift and broadening of these lines are due to quantization of the energy spectrum of excitons and can be described allowing for the steady-state size distribution of microcrystals established during their growth. We shall develop a many-band theory of the size quantization effect allowing for the nonparabolicity of the exciton subband. We shall compare the experiment and theory to find the parameters of the energy band structure of CuCl crystals.

II. INVESTIGATION OF THE DISPERSION OF THE MICROCRYSTAL SIZE

Microcrystals of CuCl were grown in the interior of a silicate glass matrix to which compounds of copper and chlorine were added in concentrations of the order of 1% (Ref. 1). The microcrystals were grown by high-temperature annealing of such glasses via diffusion-type precipitation of a new phase in a supersaturated solid solution. The microcrystal size was varied deliberately by altering the annealing

(temperature and duration) conditions. The average microcrystal radius and the concentration of the semiconducting phase in each sample were determined by the method of low-angle x-ray scattering and the approximation of monodisperse spherical particles.¹ Since the annealing temperature was higher than the melting point of CuCl, it was natural to assume that the semiconducting phase particles were liquid during growth and spherical because of the surface tension. Therefore, we postulated that the microcrystals formed as a result of solidification of such drops were indeed near-spherical.

Samples investigated in the present study were subjected to an additional low-temperature annealing. This resulted in a considerable narrowing of the exciton line and, in the final analysis, allowed us observe directly a manifestation of the size dispersion of microcrystals in the exciton luminescence spectra of these microcrystals.

§ 1. Luminescence spectra of CuCl microcrystals

Crystals of CuCl have the cubic lattice. The valence band of these crystals is split by the spin-orbit interaction into a doubly degenerate subband Γ_7 and a quadruply degenerate subband Γ_8 . In contrast to the usual diamondlike semiconductors, the Γ_7 and Γ_8 valence subbands of CuCl crystals have an inverse distribution, i.e., the doubly degenerate subband is located "above" the quadruply degenerate subband.⁶ Therefore, the exciton lines observed in the luminescence spectra of these crystals are due to the annihilation of excitons associated with the simple (only spin degenerate) valence subband Γ_7 .

Figure 1 shows the luminescence spectra of four samples containing microcrystals with different values of the average radius, recorded at $T = 4.2$ K. The luminescence was excited by a krypton-laser emission line ($\lambda = 356.4$ nm). It is clear from this figure that the spectra of the annealed samples containing microcrystals of sufficiently large size consisted of a narrow line with a maximum at $\hbar\omega = 3.178$ eV, which was due to the annihilation of an exciton bound to a neutral acceptor.⁷ The position and width of this line were practically independent of the microcrystal size and its intensity fell rapidly on increase in the size. The luminescence spectrum included also a line due to the annihilation of free

excitons. It is clear from the figure that a reduction in the microcrystal size caused this line to shift toward shorter wavelengths and, as in the case of the absorption spectra,^{2,3} this was due to the quantum size effect.

The difference between the behavior of the free and bound exciton lines was due to the fact that the wave function of a bound exciton was localized near an impurity state and was insensitive to the presence of microcrystal boundaries. Therefore, the dependences of the positions of the free- and localized-exciton lines on the microcrystal size were fundamentally different.

It is also clear from the same figure that the shift of the free-exciton line was accompanied by its considerable broadening. This broadening may be due to the dispersion of the size of microcrystals and the size distribution function can be found by analyzing the profile of the exciton line. Since this line is due to the annihilation of excitons associated with the simple valence subband, the profile can be described by the size quantization theory developed in Ref. 5.

§ 2. Exciton-line profile due to the size dispersion of microcrystals

In a quantitative analysis of the experimental results on the size quantization it is necessary to know the actual form of the size distribution function of microcrystals. This is important both to allow for the influence of the size dispersion on the optical spectra [coefficient K in Eq. (1)] and to determine the average size of microcrystals from the data on low-angle x-ray scattering.

As concluded in Ref. 1, the growth of microcrystals occurred during the recondensation stage of the process of diffusion-type precipitation of a phase in a saturated solid solution when the growth of large crystals was due to the dissolution of small ones and the concentration of the semiconducting phase remained constant. This process was discussed in greater detail in the theoretical paper of Lifshitz and Slezov,⁸ who found a function $P(a/\bar{a})$ describing the steady-state size distribution of the new particles which was established during recondensation growth. The explicit form of this function was used in Ref. 5 to obtain an expression for the exciton-spectrum intensity distribution resulting from the size variation of the microcrystals. An allowance for the "intrinsic" width of an exciton level made it possible to rewrite this expression as follows:

$$I(\omega) \sim \frac{1}{\pi a_{ex}^3} \cdot \frac{4}{3} \pi \bar{a}^3 \int_0^{\infty} du u^3 P(u) D\left(\hbar\omega - E_s + E_{ex} - \frac{\hbar^2 \pi^2}{2M\bar{a}^2} \frac{1}{u^2}\right), \quad (2)$$

$$D(x) = \frac{1}{(2\pi)^{1/2} G} \exp\left(-\frac{x^2}{2G^2}\right),$$

where $D(x)$ is a Gaussian function describing the intrinsic width G of an exciton level and the dimensionless integration variable is $u = a/\bar{a}$.

It follows therefore that the system (2) gives the position and profile of an exciton line determined by the size quantization in the case when the size distribution of the microcrystals is governed by the Lifshitz-Slezov function. It must

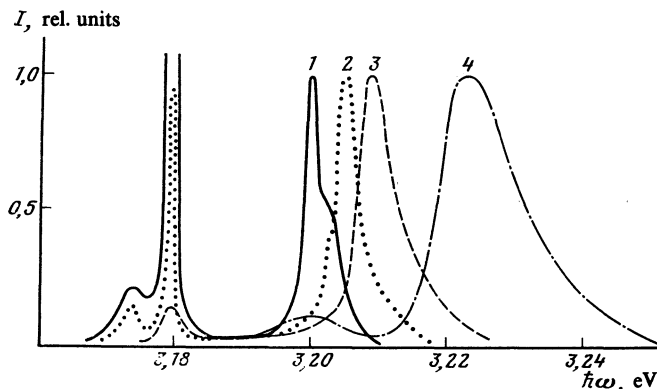


FIG. 1. Luminescence spectra of samples containing CuCl microcrystals of different radii \bar{a} (Å): 1) 140; 2) 56; 3) 45; 4) 22. $T = 4.2$ K.

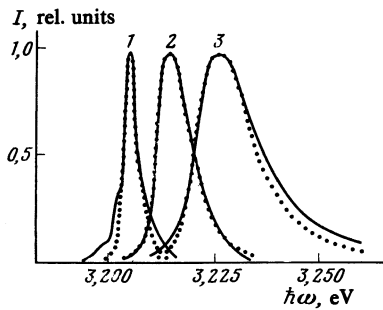


FIG. 2. Comparison of the experimental (continuous curves) and theoretical (points) profiles of the exciton luminescence lines of samples studied at $T = 4.2$ K and containing CuCl microcrystals of different radii \bar{a} (Å): 1) 56; 2) 32; 3) 22.

be stressed that the only parameter that determines the size quantization of excitons in a simple parabolic energy band is their effective mass.

Experimental profiles of the free-exciton luminescence lines determined for three samples differing in respect of the average particle radius are compared in Fig. 2 with the theoretical results obtained by numerical integration of the system (2). The best agreement was obtained for the following values of the exciton mass in Eq. (2): 1) $1.9m_0$; 2) $1.9m_0$; 3) $2.0m_0$ (m_0 is the mass of a free electron). The intrinsic width G of an exciton level does not affect the position of the exciton line maximum, but governs only its long-wavelength wing. The value of G was found to be independent of the microcrystal size and in the case of the spectra shown in Fig. 2 the best agreement was obtained for the following values: 1) $G = 1.0$ meV; 2) $G = 2.5$ meV; 3) $G = 3.5$ meV. The agreement between the experimental and calculated profiles confirmed that the size distribution of microcrystals in the investigated samples was described by the Lifshitz-Slezov distribution.

It is shown in Ref. 5 that in the case of the Lifshitz-Slezov distribution the value of the coefficient K in Eq. (1) is $K = 0.67$. Moreover, since the intensity of the scattering of x rays is proportional to the square of the volume of a microcrystal, an analysis of the results of the x-ray measurements carried out in the approximation of monodisperse particles overestimated somewhat the average microcrystal radius \bar{a} . A numerical analysis of the results of x-ray measurements carried out allowing for the size dispersion of microcrystals showed that the average (over the Lifshitz-Slezov distribution) microcrystal radius was $\bar{a} = 0.86a$, where a is the value obtained in the monodisperse approximation. The values of the coefficients found in this way were used later in an analysis of the experimental results on the quantum size shift of exciton levels.

III. SIZE QUANTIZATION OF EXCITONS IN A COMPLEX ENERGY BAND

§ 1. Experimental results

In contrast to the luminescence spectra, we found two lines in the absorption spectra of CuCl microcrystals. The long-wavelength line Z_3 was due to the creation of excitons

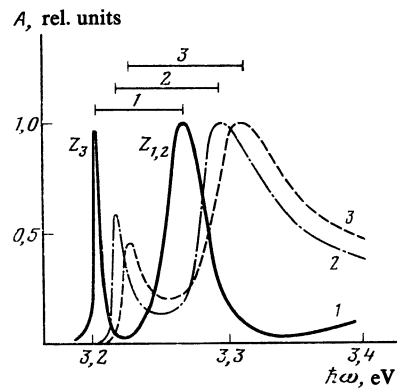


FIG. 3. Absorption spectra (here, A is the optical density) of samples containing CuCl microcrystals of different radii: 1) $\bar{a} = 270$ Å; 2) $\bar{a} = 29$ Å; 3) $\bar{a} = 22$ Å. $T = 4.2$ K.

associated with the upper doubly degenerate valence sub-band Γ_7 . The position of this line agreed resonantly, for all the microcrystal sizes, with the position of the free-exciton luminescence line considered in the preceding section. The short-wavelength line $Z_{1,2}$ was due to the excitation of excitons associated with the quadruply degenerate valence sub-band Γ_8 and the dependence of its behavior on the microcrystal size could not be described by the theory developed for a simple parabolic band.⁵

Figure 3 shows the spectra of three samples, differing in respect of the average microcrystal radius, determined at $T = 4.2$ K. Clearly, an increase in the microcrystal size resulted in a short-wavelength shift of both lines. The shift of the exciton line associated with a quadruply degenerate valence band was much stronger. We plotted in Fig. 4 (points) the positions of the maxima of both lines as a function of the reciprocal of the square of the average microcrystal radius. At high values of the radius the positions of these lines $\hbar\omega_{Z_3} = 3.201$ eV and $\hbar\omega_{Z_{1,2}} = 3.276$ eV agreed well with the published experimental data.⁶ We also used the method of least squares to plot the straight lines approximating the experimental points in Fig. 4.

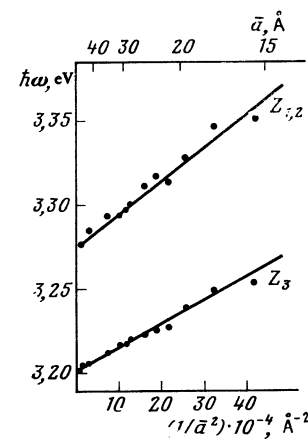


FIG. 4. Dependences of the positions of the maxima of the exciton absorption lines $Z_{1,2}$ and Z_3 at $T = 4.2$ K on the reciprocal of the square of the average radius of microcrystals.

The slope of the plot of the short-wavelength exciton-line shift associated with the upper doubly degenerate valence subband could be substituted in Eq. (1) to find, for a simple parabolic band, the effective mass of excitons which was $M = (1.9 \pm 0.2)m_0$. This value was in good agreement with the published value $M = (2.1 \pm 0.1)m_0$ (Ref. 9).

It is clear from Fig. 4 that the rate of the short-wavelength shift of the $Z_{1,2}$ line was greater than that of the Z_3 line. This was surprising because the translation mass of one of the two excitons associated with the quadruply degenerate subband was greater than for the exciton associated with the doubly degenerate subband and, consequently, the quantum

size shift of the $Z_{1,2}$ line should have been less. The results obtained could be explained only by the theory of the size quantization of excitons that allowed for the real energy band structure of CuCl crystals.

§ 2. Theory

The binding energy of excitons in CuCl is 200 meV and is considerably greater than the spin-orbit splitting $\Delta = 70$ meV. The Hamiltonian describing the translation of such an exciton in the case of low momenta p , where the kinetic energy of an exciton is much less than its binding energy, may be comparable with the value of Δ :

$$\hat{H} = \frac{1}{m_0} \begin{pmatrix} \mathcal{P} + Q & L & M & 0 & i\sqrt{1/2}L & -i\sqrt{2}M \\ L^* & \mathcal{P} - Q & 0 & M & -i\sqrt{2}Q & i\sqrt{3/2}L \\ M^* & 0 & \mathcal{P} - Q & -L & -i\sqrt{3/2}L^* & -i\sqrt{2}Q \\ 0 & M^* & -L^* & \mathcal{P} + Q & -i\sqrt{2}M^* & -i\sqrt{1/2}L^* \\ -i\sqrt{1/2}L^* & i\sqrt{2}Q & i\sqrt{3/2}L & i\sqrt{2}M & \mathcal{P} - \Delta & 0 \\ i\sqrt{2}M^* & -i\sqrt{3/2}L^* & i\sqrt{2}Q & i\sqrt{1/2}L & 0 & \mathcal{P} - \Delta \end{pmatrix}, \quad (3)$$

where

$$\begin{aligned} \mathcal{P} &= \gamma_1/2p^2, & Q &= \gamma/2(p_x^2 - 2p_z^2), & L &= -i\sqrt{3}\gamma p_x, \\ M &= \sqrt{3}/2\gamma p_x^2, & p_x^2 &= p_x^2 + p_y^2, & p_- &= p_x - ip_y, \end{aligned}$$

and the energy is measured from the position of the ground state of an exciton associated with the quadruply degenerate valence subband. This Hamiltonian is written down ignoring the electron spin, exchange electron-hole interaction, and longitudinal-transverse splitting. The numerical values of the Luttinger constants γ_1 and γ (Ref. 10) describe fully the dispersion law of the ground state of an exciton in such an energy band considered in the spherical approximation. The quantities γ_1 and γ may be associated with the values of the translation masses of excitons consisting of heavy and light holes from the Γ_8 band (M_h, M_l) and a hole from the Γ_7 band (M_s):

$$M_h = m_0/(\gamma_1 - 2\gamma), \quad M_l = m_0/(\gamma_1 + 2\gamma), \quad M_s = m_0/\gamma_1. \quad (4)$$

In fact, Eq. (3) readily yields the dispersion law of an exciton in such a band:

$$E_h = (\gamma_1 - 2\gamma)p^2/2m_0, \quad (5a)$$

$$E_{l,s} = \frac{(\gamma_1 + \gamma)}{2m_0} p^2 - \frac{\Delta}{2} \pm \left[\frac{\Delta^2}{4} + \frac{\gamma p^2}{2m_0} \Delta + 9 \left(\frac{\gamma p^2}{2m_0} \right)^2 \right]^{1/2}. \quad (5b)$$

Hence, if $\gamma p^2/m_0 \ll \Delta$, we can obtain the dispersion law of an exciton allowing for the weak nonparabolicity:

$$E_l = \frac{\gamma_1 + 2\gamma}{2m_0} p^2 + \frac{2}{\Delta} \left(\frac{\gamma p^2}{m_0} \right)^2, \quad (6a)$$

$$E_s = \frac{\gamma_1}{2m_0} p^2 - \Delta - \frac{2}{\Delta} \left(\frac{\gamma p^2}{m_0} \right)^2, \quad (6b)$$

which determines also the values of the translation masses at the bottom of the band given by Eq. (4). In the other limiting case, $\Delta \ll \gamma p^2/m_0$, we find that

$$E_l = \frac{\gamma_1 + 4\gamma}{2m_0} p^2 - \frac{\Delta}{3}, \quad E_s = \frac{\gamma_1 - 2\gamma}{2m_0} p^2 - \frac{2\Delta}{3}. \quad (7)$$

It is clear from Eqs. (6b) and (7) that an increase in the momentum p increases considerably the mass of an exciton formed from a hole in the spin-orbit split-off band.

A theory of the size quantization of excitons in semiconducting CuCl spheres can be developed assuming that the walls of a potential well are infinitely high at the well boundaries. Therefore, the wave function of an exciton on the surface of a well may be assumed to be zero. The wave functions of an exciton in a spherically symmetric well can be found if we begin by writing down the general form of spherically symmetric solutions of the Hamiltonian (3). In general, this can be done employing the results of Ref. 11. However, in describing our experiments it is sufficient (as shown below) to develop a theory of the size quantization in semiconductors with a quadruply degenerate valence band Γ_8 . In the case of an exciton associated with the band Γ_7 , a theory of its size quantization allowing for the nonparabolicity can be constructed using the Hamiltonian (3) only in the case of the states with the momentum $l = 0$, i.e., for those states which can be observed in the absorption and luminescence, in accordance with the selection rules of Ref. 5.

The Hamiltonian describing the energy spectrum of carriers at the edge of a quadruply degenerate band Γ_8 considered in the parabolic approximation can be deduced from Eq. (3) if we equate to zero the sixth and seventh columns and rows in this Hamiltonian. It is shown in Ref. 12 that spherically symmetric solutions of this Hamiltonian can be classified in accordance with the total momentum values $F = 1/2, 3/2, \dots$, which are all good quantum numbers. The states with a given value of F are $(2F + 1)$ -fold degenerate in respect of the projection of the moment M of the vector F . The wave functions of such spherically symmetric states with given F and M are¹²

$$\psi = (2F+1)^{1/2} \sum_l (-1)^{l-3/2+M} R_{F,l}(r) \sum_{m,\mu} \begin{pmatrix} l, & 3/2, & -F \\ m, & \mu, & -M \end{pmatrix} Y_{l,m}(\theta, \varphi) \chi_{\mu}, \quad (8)$$

where $Y_{l,m}(\theta, \varphi)$ are the spherical (harmonic) functions; l and m are the values of the orbital momentum and its projection; μ and χ_{μ} are the eigenvalues and the eigenvectors of the operator

$$J_z = \begin{pmatrix} 3/2 & 0 & 0 & 0 \\ 0 & 1/2 & 0 & 0 \\ 0 & 0 & -1/2 & 0 \\ 0 & 0 & 0 & -3/2 \end{pmatrix},$$

$\begin{pmatrix} a, b, c \\ e, f, g \end{pmatrix}$ are the $3j$ Wigner symbols; $M = m + \mu$; $\mu = \pm 1/2$ and $\pm 3/2$. In the case of even (relative to the coordinate origin) solutions, the wave function for given values of F and M contains two terms with l amounting to $F + 1/2$ and $F - 3/2$. Using the system of equations for $R_{3/2,l}$ from Ref. 12, we can readily show that the radial wave functions of the even states of a spherically symmetric well should have the form

$$R_{F, F+1/2} = A j_{F+1/2}(kr) + B j_{F+1/2}(kr\beta^{1/2}), \quad (9)$$

$$R_{F, F-3/2} = A' j_{F-3/2}(kr) + B' j_{F-3/2}(kr\beta^{1/2}),$$

where j_l are the modified Bessel functions related to the Bessel functions with the half-integer argument $j_l(z) = (\pi/2z)^{1/2} J_{l+1/2}(z)$; the energy of motion is

$$E = \frac{\gamma_1 - 2\gamma}{2m_0} \hbar^2 k^2; \quad A' = A \operatorname{tg} \frac{\alpha_F}{2},$$

$$B' = -B \operatorname{ctg} \frac{\alpha_F}{2}; \quad \cos \alpha_F = \frac{2F-3}{4},$$

whereas the ratio of the masses of the light and heavy particles is $\beta = (\gamma_1 - 2\gamma)/(\gamma_1 + 2\gamma)$. The vanishing of the wave function of an exciton at the boundary of a sphere of radius a yields the following system of equations for the determination of the energy levels:

$$R_{F, F+1/2}(a) = A j_{F+1/2}(k_F, n a) + B j_{F+1/2}(k_F, n a \beta^{1/2}) = 0, \quad (10)$$

$$R_{F, F-3/2}(a) = A \operatorname{tg} \frac{\alpha_F}{2} j_{F-3/2}(k_F, n a) - B \operatorname{ctg} \frac{\alpha_F}{2} j_{F-3/2}(k_F, n a \beta^{1/2}) = 0,$$

which can be solved if

$$j_{F+1/2}(k_F, n a) j_{F-3/2}(k_F, n a \beta^{1/2}) + \frac{6F-3}{2F+3} j_{F-3/2}(k_F, n a) j_{F+1/2}(k_F, n a \beta^{1/2}) = 0. \quad (11)$$

We have used here the relationship

$$\operatorname{tg}^2(\alpha_F/2) = (2F+3)/(6F-3).$$

Solving Eq. (11) for $k_{F,n}$ and then using the relationship between E and k , we can find the energy levels

$$E_{F,n} = \frac{\gamma_1 - 2\gamma}{2m_0} \hbar^2 k_{F,n}^2, \quad (12)$$

where n is the serial number of the root of Eq. (11) for a given

value of F . As in the case of a simple parabolic band, the value of $k_{F,n}$ can be represented in the form

$$k_{F,n} = \varphi_n^F / a, \quad (13)$$

where φ_n^D is the set of numerical coefficients dependent on the ratio of the masses of light and heavy quasiparticles $\beta = M_l/M_h$. In the case when $\beta = 1$ ($\gamma = 0$), the set of numbers φ_n^F is identical with the roots of the Bessel functions $\varphi_{l,n}$ (Ref. 5) (here, n is the serial number of the root of a modified Bessel function j_l with $l = F - 3/2$), exactly as in the case of a simple parabolic band. If $\beta \ll 1$, we can expand the Bessel functions with small arguments as a series in Eq. (11) and this gives

$$j_{F+1/2}(\varphi_n^F) \approx -\frac{6F-3}{2F+3} \left(\frac{\varphi_n^F}{2} \right)^2 \beta \frac{1}{F(F+1)} j_{F-3/2}(\varphi_n^F) \xrightarrow{\beta \rightarrow 0} 0. \quad (14)$$

Hence, it is clear that when the difference between the masses is large so that $M_l \ll M_h$, the numbers φ_n^F are again identical with the roots of a Bessel function j_l shifted in respect of the momentum l by 2, i.e., with $\varphi_{F+1/2,n}^F$. For small values of F and n this may increase considerably the roots of φ_n^F on reduction in β . For example, for excitons with the momentum $F = 3/2$ (which are the only ones that contribute to the exciton absorption in CuCl) the first root of Eq. (11) for $F = 3/2 - \varphi_1^{3/2}$ varies approximately from 3.14 to 5.76, i.e., it varies almost twofold.

We shall now consider how the influence of the many-band nature of the Hamiltonian (3) affects the size quantization levels of excitons associated with the valence subband Γ_7 . The general form of the wave function of an exciton described by the Hamiltonian (3) in a spherically symmetric potential well is as follows for the states with the momentum $l = 0$ (Ref. 11):

$$\psi = \begin{cases} R_h \begin{pmatrix} -Y_{2,-1} \\ \sqrt{2i} Y_{2,0} \\ \sqrt{3} Y_{2,1} \\ -2i Y_{2,2} \end{pmatrix}, \\ R_s \begin{pmatrix} Y_{0,0} \\ 0 \end{pmatrix} \end{cases},$$

where $R_h(r)$ and $R_s(r)$ are the radial wave functions for which we can obtain the following system of equations if we substitute Eq. (15) into Eq. (3):

$$\begin{aligned} & \left[\frac{\gamma_1 + 2\gamma}{2} \left(\frac{1}{r^2} \frac{\partial}{\partial r} r^2 \frac{\partial}{\partial r} - \frac{6}{r^2} \right) + \varepsilon \right] R_h \\ & + \sqrt{2} \gamma \left(\frac{d}{dr} - \frac{1}{r} \right) \frac{d}{dr} R_s = 0, \\ & \sqrt{2} \gamma \left(\frac{d}{dr} + \frac{2}{r} \right) \left(\frac{d}{dr} + \frac{3}{r} \right) R_h \\ & + \left(\frac{\gamma_1}{2} \frac{1}{r^2} \frac{\partial}{\partial r} r^2 \frac{\partial}{\partial r} + \varepsilon + \delta \right) R_s = 0, \end{aligned} \quad (16)$$

where $\varepsilon = m_0 E / \hbar^2$, $\delta = m_0 \Delta / \hbar^2$. Its solutions are the Bessel functions

$$R_h(r) = C_h j_2(kr), \quad R_s(r) = C_s j_0(kr), \quad (17)$$

and the coefficients C_h and C_s are related by the following system of equations:

$$\begin{aligned} [\varepsilon^{-1/2}(\gamma_1+2\gamma)k^2]C_h + \sqrt{2}\gamma k^2 C_s &= 0, \\ \sqrt{2}\gamma k^2 C_h + (\varepsilon + \delta^{-1/2}\gamma_1 k^2)C_s &= 0. \end{aligned} \quad (18)$$

The condition for the solubility of the system (18) is given by the dispersion law of excitons, identical with Eq. (6b). On the other hand, for each value of the energy E there are two solutions of the (17) type differing in respect of k . In the energy range $-\Delta < E < 0$ one of these values is imaginary and the square of the absolute value of $k_{s,h}$ is

$$\begin{aligned} k_{s,h}^2 &= \frac{m_0}{\hbar^2(\gamma_1-2\gamma)(\gamma_1+4\gamma)} |2E(\gamma_1+\gamma) + \Delta(\gamma_1+2\gamma) \\ &\pm \{[2E(\gamma_1+\gamma) + \Delta(\gamma_1-2\gamma)]^2 - 4E(E+\Delta)(\gamma_1-2\gamma)(\gamma_1+4\gamma)\}^{1/2}. \end{aligned} \quad (19)$$

Then, the radial components of the wave functions of an exciton considered in this energy range are

$$\begin{aligned} R_h(r) &= C_h^s j_2(k_s r) + C_h^h I_2(k_h r), \\ R_s(r) &= C_s^s j_0(k_s r) + C_s^h I_0(k_h r), \end{aligned} \quad (20)$$

where $I_l(z)$ are the modified Bessel functions with the complex argument, whereas the coefficients C_a^b are related by

$$\begin{aligned} C_h^s &= -(\varepsilon + \delta^{-1/2}\gamma_1 k_s^2) / \sqrt{2}\gamma k_s^2 C_s^s, \\ C_h^h &= -(\varepsilon + \delta^{+1/2}\gamma_1 k_h^2) / \sqrt{2}\gamma k_h^2 C_s^h. \end{aligned} \quad (21)$$

Using next the boundary condition $R_h(a) = R_s(a) = 0$, we obtain the following equation for determination of the size quantization levels:

$$\begin{aligned} j_0(k_s a) I_2(k_h a) - j_2(k_s a) I_0(k_h a) \\ \times (\varepsilon + \delta^{-1/2}\gamma_1 k_s^2) k_h^2 / (\varepsilon + \delta^{+1/2}\gamma_1 k_h^2) k_s^2 = 0. \end{aligned} \quad (22)$$

We shall consider the case of a weak nonparabolicity when $\gamma k_s^2 \hbar^2 / m_0 \ll \Delta$. However, we have $k_h a \gg 1$ and $I_2(k_h a) / I_0(k_h a) \rightarrow 1$. Next, applying the expansion (6b), we readily obtain from Eq. (22) that

$$j_0(k_s a) = -\frac{4\hbar^2 k_s^2 \gamma^2}{m_0 \Delta \gamma_1} j_2(k_s a) = \alpha \ll 1. \quad (23)$$

We shall solve this equation by the method of successive approximations. We shall find first the root of the equation

$$j_0(k_s a) = j_0(\varphi) = 0. \quad (24)$$

For the ground state this root is $\varphi^0 = k_s^0 a = \pi$. Next, we obtain the correction to this root:

$$\Delta\varphi = \alpha \left(\frac{\partial j_0}{\partial \varphi} \right)_\pi^{-1} = -\frac{4\pi^2 \gamma^2 \hbar^2}{a^2 m_0 \gamma_1 \Delta} j_2(\pi) \left(\frac{\partial j_0}{\partial \varphi} \right)_\pi^{-1} = \frac{12\pi^2 \gamma^2 \hbar^2}{\gamma_1 m_0 a^2} \frac{1}{\Delta}, \quad (25)$$

which gives $\Delta k_s = 12\pi^2 \hbar^2 / \gamma_1 m_0 a^3 \Delta$. Substituting the value of Δk_s into the expansion (6b), we obtain the correction to the size quantization levels of an exciton formed from a hole in the Γ_7 band and related to its nonparabolicity:

$$\begin{aligned} E &\approx -\Delta + \frac{\gamma_1 \hbar^2 k_s^2}{2m_0} - \frac{2}{\Delta} \left(\frac{\gamma \hbar^2 k_s^2}{m_0} \right)^2 \\ &\approx -\Delta + \frac{\gamma_1 \hbar^2 (k_s^0)^2}{2m_0} + \gamma \frac{\hbar^2}{m_0} k_s^0 \Delta k_s \\ &- \frac{2}{\Delta} \left[\frac{\gamma \hbar^2 (k_s^0)^2}{m_0} \right]^2 = -\Delta + \frac{\gamma_1 \hbar^2 \pi^2}{2m_0 a^2} - \frac{2}{\Delta} \left(\frac{\gamma \hbar^2 \pi^2}{m_0 a^2} \right)^2 \left(1 - \frac{6}{\pi^2} \right). \end{aligned} \quad (26)$$

Therefore, the nonparabolicity of the exciton spectrum should be manifested as a deviation from the linear dependence of the short-wavelength shift of the exciton line on $1/a^2$.

§ 3. Discussion of results

In the preceding subsection we found theoretically the quantum-size shift of the exciton lines associated with the subbands Γ_7 and Γ_8 of a semiconductor sphere of radius a , described by Eqs. (28) and (12) or (13), respectively. The experimental results agree with these formulas if we allow for the dispersion of the size of the spheres. We found experimentally (see Sec. II) that the distribution of the particle size of such heterophase systems grown by recondensation is described by the Lifshitz-Slezov function.⁸ Then, allowing for the dispersion of the size of the spheres in the way it was done in Ref. 5, we can determine the dependence of the profile and positions of both exciton lines on the radius \bar{a} averaged over the distribution. In the case of excitons associated with the valence subband Γ_7 the position of the line maximum is described by the expression

$$\hbar\omega_{z_s} = E_g - E_{ex} + 0.67 \frac{\gamma_1 \hbar^2 \pi^2}{2m_0 \bar{a}^2} - \frac{0.46}{\Delta} \left(\frac{\gamma \hbar^2 \pi^2}{m_0 \bar{a}^2} \right)^2 2 \left(1 - \frac{6}{\pi^2} \right). \quad (27)$$

Here, the last term proportional to $1/\bar{a}^4$ allows for the exciton spectrum nonparabolicity. We also see from Fig. 4 that the short-wavelength shift is a practically linear function of $1/\bar{a}^2$. Hence, it follows that the nonparabolicity of the excitons associated with the subband Γ_7 of CuCl is weak. Therefore, the exciton line shift is the same as for a simple parabolic energy band with an effective mass $M_s = m_0/\gamma_1$.

The position of the maximum of the exciton line associated with the valence subband Γ_8 depends as follows on \bar{a} :

$$\hbar\omega_{z_{1,2}} = E_g + \Delta - E_{ex} + 0.67 \hbar^2 \frac{\gamma_1 - 2\gamma}{2m_0 \bar{a}^2} (\varphi_1^{3/2})^2. \quad (28)$$

Therefore, the short-wavelength shift of such an exciton with a fourfold degeneracy of the energy spectrum at $k = 0$ is, as expected, inversely proportional to its "heavy" mass $M_h = m_0/(\gamma_1 - 2\gamma)$. However, the dependence on the energy band parameters includes also $\varphi_1^{3/2}$ representing the first root of Eq. (11) corresponding to $F = 3/2$:

$$j_2(\varphi^{3/2}) j_0(\varphi^{3/2} \beta^{1/2}) + j_0(\varphi^{3/2}) j_2(\varphi^{3/2} \beta^{1/2}) = 0. \quad (29)$$

Here, the parameter $\beta = (\gamma_1 - 2\gamma)/(\gamma_1 + 2\gamma)$ depends on the ratio γ/γ_1 . Equation (29) replaces the corresponding equation $j_0(\varphi) = 0$ for a simple energy band and, therefore, in the case of a complex band the value of $\varphi_1^{3/2}$ replaces the first root of the Bessel function $j_0(x)$, which is the number π in Eqs. (1) and (27).

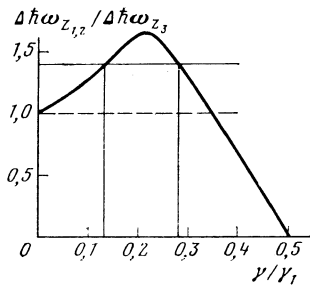


FIG. 5. Dependence of the ratio of the shifts of the exciton absorption lines $Z_{1,2}$ and Z_3 on the value of γ/γ_1 .

In an analysis of the experimental results it is convenient to use not the absolute shift of the exciton lines

$$\Delta\hbar\omega_{Z_3}(\bar{a}) = \hbar\omega_{Z_3}(a) - E_g + E_{ex},$$

$$\Delta\hbar\omega_{Z_{1,2}}(\bar{a}) = \hbar\omega_{Z_{1,2}}(\bar{a}) - E_g - \Delta + E_{ex},$$

but the ratio of the shifts which, in the parabolic approximation, is of the form [see Eqs. (27) and (28)]

$$\frac{\Delta\hbar\omega_{Z_{1,2}}(\bar{a})}{\Delta\hbar\omega_{Z_3}(\bar{a})} = \frac{\gamma_1 - 2\gamma}{\gamma_1} \left(\frac{\varphi_1^{3/2}}{\pi} \right)^2, \quad (30)$$

i.e., it is independent of the microcrystal size and is governed only by the ratio of the band parameters γ/γ_1 . Figure 5 shows a theoretical plot of this dependence. We found numerically the first root $\varphi_1^{3/2}$ of Eq. (29). It is clear from this figure that the short-wavelength shift $\Delta\hbar\omega_{Z_{1,2}}$ of the excitons associated with the valence subband Γ_8 is, because of the coefficient $\varphi_1^{3/2}$, greater than $\Delta\hbar\omega_{Z_3}$ right up to $\gamma/\gamma_1 \approx 0.35$. This is why the slope of the dependence $\hbar\omega_{Z_{1,2}}(\bar{a})$ in Fig. 4 is greater than that of $\hbar\omega_{Z_3}(\bar{a})$.

Figure 4 can be used to find the ratio of the short-wavelength shifts $\Delta\hbar\omega_{Z_{1,2}}/\Delta\hbar\omega_{Z_3} = 1.4$. It is clear from Fig. 5 that this ratio corresponds to either $\gamma/\gamma_1 = 0.13$ or $\gamma/\gamma_1 = 0.28$. We can use the mass $M_s = 1.9m_0$ of the excitons associated with the valence subband Γ_7 , which corresponds to $\gamma_1 = 0.53$, and thus obtain two alternative values of the constant γ : $\gamma = 0.07$ or $\gamma = 0.15$. It is clear from Eq. (27) that the value of γ determines the degree of nonparabolicity of the exciton band associated with the Γ_7 valence subband and this makes it possible to select one of the values of γ by comparison with the experimental results. Figure 6 shows the dependences of the short-wavelength line shift Z_3 on the reciprocal of the square of the average radius of microcrystals plotted for both values of γ . We can see that $\gamma = 0.07$ indeed corresponds to a weak nonparabolicity and describes better the experimental points.

The values of the Luttinger parameters $\gamma_1 = 0.53 \pm 0.06$ and $\gamma = 0.070 \pm 0.007$ obtained in this way from Eq. (4) can be used to determine the translation masses of exci-

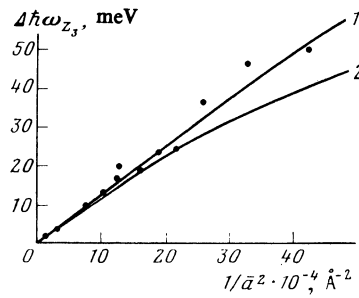


FIG. 6. Theoretical dependence of the position of the Z_3 line on the reciprocal of the square of the average radius of microcrystals, plotted allowing for the nonparabolicity of the exciton energy band. The curves correspond to different values of the parameter γ : 1) 0.07; 2) 0.15. The experimental results obtained at 4.2 K are represented by points.

tons. For the excitons associated with the upper valence subband Γ_7 , the mass is $M_s = (1.9 \pm 0.2)m_0$, in good agreement with the published data.⁹ The excitons associated with the quadruply degenerate subband Γ_8 are characterized by the masses $M_h = (2.6 \pm 0.2)m_0$ and $M_l = (1.5 \pm 0.2)m_0$, which—to the best of our knowledge—were determined by us for the first time.

It is therefore clear that an investigation of the dependences of the positions of the exciton lines on the size of microcrystals makes it possible to study the dispersion law of excitons in a wide range of values of the quasimomentum and it provides a new method for investigating the energy band structure of semiconductor crystals.

The authors are deeply grateful to A. L. Éfros for valuable discussions.

¹V. V. Golubkov, A. I. Ekimov, A. A. Onushchenko, and V. A. Tsekhomskii, *Fiz. Khim. Stekla* **7**, 397 (1981).

²A. I. Ekimov and A. A. Onushchenko, *Pis'ma Zh. Eksp. Teor. Fiz.* **34**, 363 (1981). [*JETP Lett.* **34**, 345 (1981)].

³A. I. Ekimov and A. A. Onushchenko, *Fiz. Tekh. Poluprovodn.* **16**, 1215 (1982) [*Sov. Phys. Semicond.* **16**, 775 (1982)].

⁴A. I. Ekimov and A. A. Onushchenko, *Trudy Vsesoyuznoĭ konferentsii po fizike poluprovodnikov* (Proc. All-Union Conf. on Physics of Semiconductors), Baku, 1982, p. 176; *Pis'ma Zh. Eksp. Teor. Fiz.* **40**, 337 (1984) [*JETP Lett.* **40**, 1136 (1984)].

⁵A. L. Éfros and A. L. Éfros, *Fiz. Tekh. Poluprovodn.* **16**, 1209 (1982) [*Sov. Phys. Semicond.* **16**, 772 (1982)].

⁶A. Goldmann, *Phys. Status Solidi B* **81**, 9 (1977).

⁷M. Certier, C. Wecker, and S. Nikitine, *J. Phys. Chem. Solids* **30**, 2135 (1969).

⁸I. M. Lifshitz and V. V. Slezov, *Zh. Eksp. Teor. Fiz.* **35**, 479 (1958) [*Sov. Phys. JETP* **8**, 331 (1959)].

⁹Y. Masumoto, Y. Unuma, Y. Tanaka, and S. Shionoya, *J. Phys. Soc. Jpn.* **47**, 1844 (1979).

¹⁰J. M. Luttinger, *Phys. Rev.* **102**, 1030 (1956).

¹¹V. I. Sheka and D. I. Sheka, *Zh. Eksp. Teor. Fiz.* **51**, 1445 (1966) [*Sov. Phys. JETP* **24**, 975 (1967)].

¹²B. L. Gel'mont and M. I. D'yakov, *Fiz. Tekh. Poluprovodn.* **5**, 2191 (1971) [*Sov. Phys. Semicond.* **5**, 1905 (1972)].

Translated by A. Tybulewicz

Quantization of the energy spectrum of holes in the adiabatic potential of the electron

A. I. Ekimov, A. A. Onushchenko, and Al. L. Éfros

A. F. Ioffe Physicotechnical Institute, Academy of Sciences of the USSR

(Submitted 31 January 1986)

Pis'ma Zh. Eksp. Teor. Fiz. **43**, No. 6, 292–294 (25 March 1986)

The spectra of the interband absorption of microscopic CdS crystals, 15 to 30 Å in size, grown in a transparent insulating matrix, are analyzed. A structural feature caused by quantization of the energy spectrum of the hole in the adiabatic potential of its Coulomb interaction with the electron has been detected near the transitions to the lower level of the size quantization of the electron.

Several years ago, a technique was developed for growing microscopic semiconductor crystals in the bulk of a transparent insulating glass matrix, in which their size can be varied directionally over a broad range from several tens to several thousands of angstroms.^{1,2} Quantum size effects in the energy spectrum of excitons^{3,4} and electrons^{2,5} were detected in such heterophase systems by the methods of optical spectroscopy. In the present letter we report the observation of a quantum size effect, theoretically predicted by Éfros and Éfros,⁶ in the energy spectrum of holes in a potential well which results from the electron charge density distribution in the microscopic crystal.

Figure 1 shows a spectrum of the interband absorption of microscopic CdS crystals with a mean radius $\bar{a} \approx 20$ Å, which was measured at $T = 4.2$ K, and the spectra of the second derivative $\partial^2 A / \partial \lambda^2$, which were measured at $T = 4.2, 77,$ and 300 K. The average size of the microscopic crystals was measured by the method of small-angle scattering of x-rays.¹ The large-scale oscillations observed in the spectra are caused, as was shown elsewhere,⁵ by the transitions to the electron size quantization levels in the conduction band. This figure shows that a structure, clearly seen in the spectra of the second derivative at $T = 4.2$ and 77 K, manifests itself at low temperatures in the spectral region of the transitions to the first level of electron size quantization. As the temperature is raised, this structure becomes diffuse, and at room temperature it cannot be resolved at all even in the spectra of the second derivative. A similar situation occurs in the range of values of the microscopic-crystal radii $15 \text{ Å} \leq \bar{a} \leq 23 \text{ Å}$, which are smaller than the exciton radius ($r_{\text{exc}} = 30 \text{ Å}$) in CdS crystals. The magnitude of the splitting, which depends on the size of the microscopic crystals, increases with decreasing \bar{a} .

As was shown theoretically in Ref. 6, this effect can be attributed to the Coulomb interaction of an electron-hole pair produced as a result of absorption of a light quantum. In the range of microscopic-crystal sizes $a < r_{\text{exc}}$, the energy of motion of an electron in a quantum well is in fact considerably higher than the energy of the Coulomb interaction of the quantum well with the hole. In the case of semiconducting materials with $m_e \ll m_h$ (m_e and m_h are the effective masses of the electron and the hole), the Coulomb potential of the electron which affects the hole may therefore be assumed averaged over the fast motion of the electron (adiabatic approximation). If

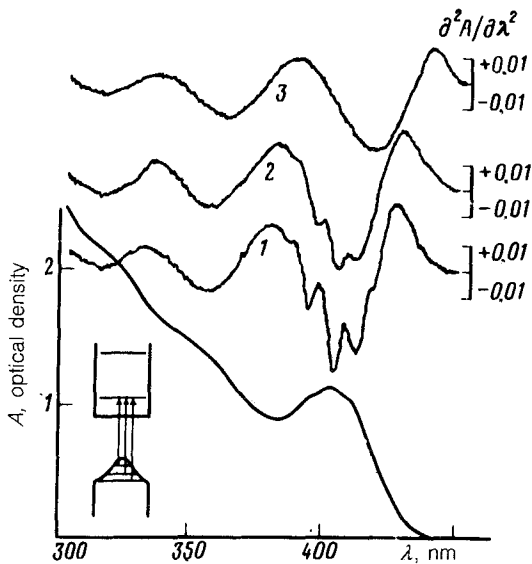


FIG. 1. Spectrum of interband absorption of microscopic CdS crystals ($a = 20 \text{ \AA}$) at $T = 4.2 \text{ K}$ and spectra of the second derivative $\partial^2 A / \partial \lambda^2$ at (1) $T = 4.2 \text{ K}$, (2) $T = 77 \text{ K}$, and (3) $T = 300 \text{ K}$.

the electron is situated at the lower size-quantization level, this potential will have a minimum at the center of the semiconducting sphere and near the bottom we can write the potential in the form⁶

$$V(r_h) = -\alpha \frac{e^2}{\kappa a} + \frac{\pi^2}{3} \frac{e^2}{\kappa a} \frac{r_h^2}{a^2}; \quad r_h \ll a, \quad (1)$$

where κ is the dielectric constant of the crystal, the numerical factor $\alpha = 2 \int_0^\pi dy \sin^2 y / y \approx 2.4$ takes into account the electron charge density distribution at this level, and r_h^0 is the distance by which the hole is displaced from the center of the sphere. As we can see in Fig. 1, allowance for the Coulomb interaction in the microscopic crystals with a radius smaller than the exciton radius ($a < r_{\text{exc}}$) leads to the appearance in the hole of an additional potential well of depth on the order of $e^2/\kappa a$.

The role played by the additional potential well in the formation of the energy spectrum of the holes is determined essentially by the ratio of the well depth and the energy of the size quantization of the holes in the microscopic crystal. The relative contribution of these quantities, which depends on the size of the microscopic crystals, can be estimated in order of magnitude. It can easily be shown that the energy of the Coulomb interaction $\sim e^2/\kappa a$ is higher than the energy of the size quantization of the holes, $\sim \hbar^2/m_h a^2$, if the microscopic-crystal radii satisfy the condition

$$a > \frac{\kappa \hbar^2}{m_h e^2} \equiv a_h,$$

where a_h is the Bohr radius of the hole. For most of the semiconducting materials $a_h \lesssim 10 \text{ \AA}$ and this condition is satisfied down to the smallest realistically attainable sizes of the microscopic crystals. In semiconducting materials with $m_c \ll m_h$, the energy

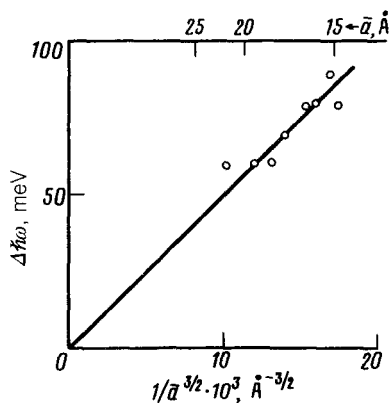


FIG. 2. Experimental dependence of the splitting on the size of the microscopic crystals.

spectrum of the holes is thus determined by the electron-motion-averaged potential of the Coulomb interaction, rather than by the size quantization of the holes in the potential well of the microscopic crystal, as was assumed in Ref. 7.

Since the condition $m_e \ll m_h$ is satisfied for CdS crystals, and since the Bohr radius is no greater than $a_h \lesssim 7 \text{ \AA}$, the energy spectrum of the holes for the sizes under study must be determined by the potential of the Coulomb interaction of the hole with the electron. As we can see from (1), this potential has the form of the potential of a three-dimensional harmonic oscillator. The motion of a hole in such a potential leads to the appearance in its energy spectrum of an equally spaced series of lines whose spacing is determined by⁶

$$\Delta \hbar \omega_h = \left(\frac{8}{3} \frac{e^2}{\kappa a} \frac{\hbar^2 \pi^2}{m_h a^2} \right)^{1/2}. \quad (2)$$

The wave functions of the holes which correspond to these states differ markedly from the wave functions which describe their motion in the absence of Coulomb interaction. As a result, the selection rules change and the optical transitions from each level to a lower size-quantization level become resolved.⁶ This circumstance accounts for the appearance of a structure in the spectrum of the interband transitions to the first level on the size quantization of the electron (see the inset in Fig. 1).

Figure 2 is a plot of the experimental curve for the splitting, $\Delta \hbar \omega$, versus the mean radius of the microscopic crystals \bar{a} . We see that the splitting is proportional to $\bar{a}^{-3/2}$, consistent with (2). The phenomenon which we have observed can thus be qualitatively described in terms of a very simple model which takes into account the interaction of an electron with the hole in a simple parabolic zone. A quantitative analysis of the experimental results cannot, however, be carried out without the use of a theory which takes the actual structure of the valence band of CdS into account.

Our results thus show that for a size of the microscopic crystals in the range $r_{\text{exc}} < a < a_h$ the Coulomb interaction leads to the appearance of an additional potential well which determines the energy spectrum of the holes in the microscopic crystal. A

similar phenomenon should also occur in quasi-two-dimensional structures with quantum wells.

- ¹V. V. Golubkov, A. I. Ekimov, A. A. Onushchenko, and V. A. Tsekhomskii, *Fiz. i khim. stekla* **7**, 397 (1981).
- ²A. I. Ekimov and A. A. Onushchenko, Proceedings of the All-Union Conference on the Physics of Semiconductors, Baku, 1982, p. 176.
- ³A. I. Ekimov and A. A. Onushchenko, *Pis'ma Zh. Eksp. Teor. Fiz.* **34**, 363 (1981). [*JETP Lett.* **34**, 345 (1981)].
- ⁴A. I. Ekimov, A. A. Onushchenko, A. G. Plyukhin, and Al. L. Éfros, *Zh. Eksp. Teor. Fiz.* **88**, 1490 (1985) [*Sov. Phys. JETP* **61**, 891 (1985)].
- ⁵A. I. Ekimov and A. A. Onushchenko, *Pis'ma Zh. Eksp. Teor. Fiz.* **40**, 337 (1984) [*JETP Lett.* **40**, 1136 (1984)].
- ⁶A. L. Éfros and A. L. Éfros, *Fiz. Tekh. Poluprovodn.* **16**, 1209 (1982) [*Sov. Phys. Semicond.* **16**, 772 (1982)].
- ⁷L. E. Brus, *J. Chem. Phys.* **80**, 4403 (1984).

Translated by S. J. Amoretty

Proc. XIX International School of Semiconducting Compounds, Jaszowiec 1990

OPTICS OF ZERO DIMENSIONAL SEMICONDUCTOR SYSTEMS

A.I. EKIMOV AND AL.L. EFROS

S.I. Vavilov State Optical Institute, 199164 Leningrad, USSR

(Received August 8, 1990)

The optical spectra of semiconductor microcrystals grown in transparent matrix of oxide glass are investigated. The size of microcrystals was varied in a controlled manner from a few tens to a few hundreds of angstroms. The microcrystal embedded in wide gap matrix represents three-dimensional potential well for electrons, holes and excitons. The optical properties of such zero-dimensional semiconductor structures are shown to be governed by the structure of energy spectra of confined electron-hole pairs. The phenomenon of the microcrystals ionization at interband optical excitation is observed. The Auger process in microcrystals containing two nonequilibrium electron-hole pairs is proposed to be responsible for this effect. The experimental dependencies of the ionization rate as a function of excitation intensity and the microcrystal size are in a good agreement with the theoretical predictions of the Auger recombination model.

PACS numbers: 78.90.+t

Optics of semiconductor microcrystals embedded in dielectric matrices have been a subject of very intensive investigations for the last years [1, 2]. Actually, there are two reasons for this. The first reason is a fundamental character of phenomena which dominate the energy spectrum of electronic states in microcrystals. It is well established now that a semiconductor microcrystal in a wide-band matrix represents a three-dimensionally confined quantum well for quasiparticles. When microcrystals have sizes comparable to the Bohr radius of the exciton in the bulk semiconductor the resulting quantum confinement strongly modifies the optical spectra. The second reason is possible device applications which are due to the expected largely enhanced optical nonlinearities [3] and electro-optical effects [4] in semiconductor-doped glasses.

The purpose of this talk is to give a short review of the present situation in the studies of the zero-dimensional semiconductor systems. The growth technique and optical spectra of microcrystals in a glass matrix will be discussed at some length. Another problem to be discussed is the energy spectra of zero-dimensionally

confined electron-hole pairs in quantum semiconductor dots. And finally, the role of Auger-processes in photoionization of semiconductor microcrystals in a glass matrix will be regarded.

1. Semiconductor microcrystals in a glass matrix: growth and optical spectra

The developed technologies make it possible to grow the microcrystals of semiconductor compounds in glassy [5], crystalline [6] and aqueous matrices [7]. The growth of microcrystals in solid matrices is based on the process of diffusion – controlled phase decomposition of a super saturated solid solution. The recondensation stage of the process, when the large particles grow at the expense of dissolution of small ones, was investigated theoretically by Lifshits and Slesov. The kinetics of growth is described by the following expression [8]

$$\bar{a} = \left(\frac{4}{9} \sigma C D \tau \right)^{\frac{1}{3}} \quad (1)$$

where the diffusion coefficient D and equilibrium concentration of the solution C depend exponentially on temperature; σ is a coefficient proportional to interfacial surface tension, τ – time duration of annealing process. Mean value of the microcrystal radius may be measured off small-angle X-ray scattering [5] or with the use of TEM technique [9]. It was also shown that a steady-state size distribution is formed in the course of recondensation growth and an analytical expression for it was obtained [8].

Thus, the technique of diffused-controlled growth of semiconductor microcrystals makes it possible to vary the size of particles starting from a few tenths of angstroms. The steady-state size distribution of microcrystals is rather narrow and may be taken into account in calculations, since the analytical expression for it is known. Further investigations of the growth process are in progress now. A biosynthesis of CdS microcrystals was announced recently [10]. Sol-gel technology of silicate glass production was shown to be useful for microcrystals growth [11]. The Ge microcrystals embedded in SiO₂ thin films were obtained with rf sputtering technique [12].

The optical transparency of an oxide glass matrix makes it possible to apply all of the methods of optical spectroscopy to study such zero-dimensional system. The Figure 1 shows the absorption spectra of glass samples containing CdSe, CdS, CuBr and CuCl microcrystals. It is seen that spectra reveal the typical excitonic structure of near band-gap transitions. This structure is due to the spin-orbit splitting in cubic materials (CuBr, CuCl) and to the spin-orbit and crystal field splitting in hexagonal semiconductors (CdS, CdSe). The absorption spectra as well as luminescence and Raman spectra show that the semiconductor particles grown in glass matrix have the crystalline structure and sufficiently high spectroscopic quality. The X-ray scattering experiments were carried out recently for investigation of structural modifications of CdS [10] and CdSe [13] microcrystals.

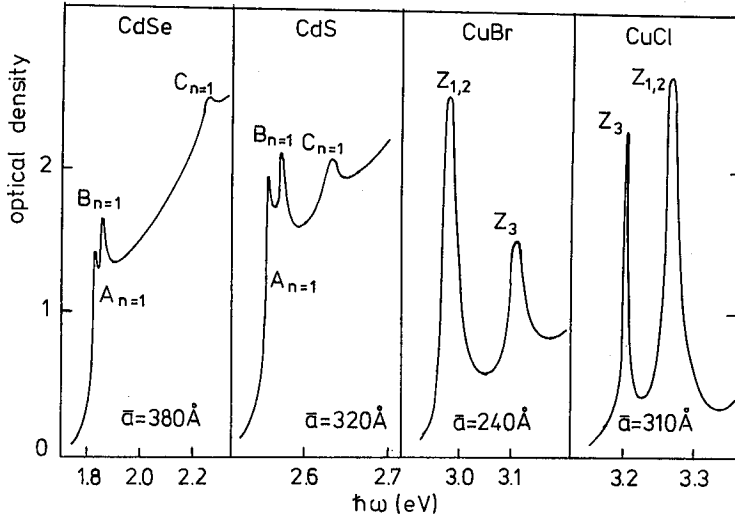


Fig.1. Low temperature ($T = 4.2$ K) absorption spectra of glasses with microcrystals: CdSe ($\bar{a} = 380$ Å), CdS ($\bar{a} = 320$ Å), CuBr ($\bar{a} = 240$ Å), and CuCl ($\bar{a} = 310$ Å).

2. Energy spectrum of electronic states in semiconductor quantum dots

The semiconductor-doped glasses are of interest as a new class of objects which may be used for the investigation of quantum confined effects in semiconductors. Besides size quantization, the spectra of electron-hole pairs are also influenced by the Coulomb interaction, the energy of which depends on microcrystal size too. So, the different cases, depending on relationship between these two energies have to be regarded.

The Figure 2a shows the absorption spectra of glasses doped with CuCl microcrystals of different sizes. As can be seen, the absorption is of excitonic nature down to smallest sizes. The decrease of the radius of microcrystals leads to high blue shift for both excitonic lines. This effect is due to the size quantization of an exciton as a whole, because the binding energy of the exciton in the material is very high ($E_{ex} \approx 0.2$ eV) and the radius of exciton is rather small ($r_{ex} \approx 8$ Å). The size dependence of spectral position of both excitonic lines are shown in Fig. 2b. For the exciton originating from the upper, nondegenerate subband Γ_7 the dependence is described by simple expression

$$\hbar\omega_{Z_s} = E_g - E_{ex} + 0.67 \frac{\hbar^2}{2M_s \bar{a}^2} \pi^2 \quad (2)$$

where E_g is the band gap and E_{ex} is the exciton binding energy. The numerical factor results from the averaging of the Lifshits size distribution function. The slope of the curve is determined by the value of the excitonic translation mass M_s .

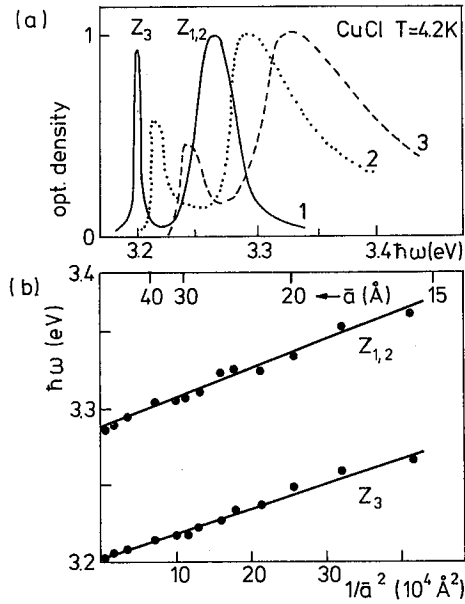


Fig.2. (a) Absorption spectra of glasses with CuCl microcrystals: (1) $\bar{a} = 310 \text{ \AA}$, (2) $\bar{a} = 29 \text{ \AA}$, (3) $\bar{a} = 20 \text{ \AA}$. (b) Spectral position of oscillations vs. $1/\bar{a}^2$.

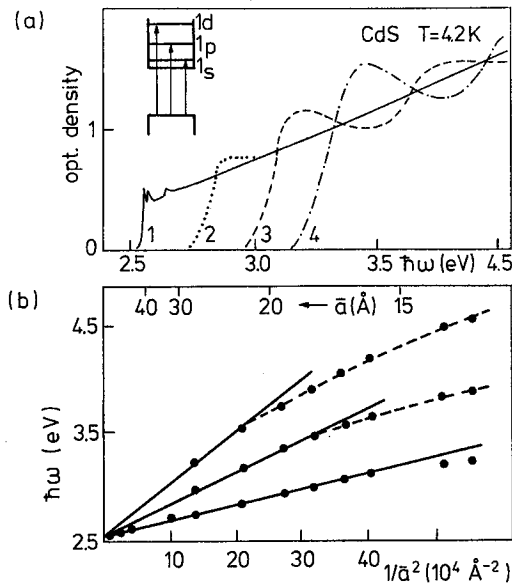


Fig.3. (a) Absorption spectra of glasses with CdS microcrystals: (1) $\bar{a} = 330 \text{ \AA}$, (2) $\bar{a} = 23 \text{ \AA}$, (3) $\bar{a} = 15 \text{ \AA}$, (4) $\bar{a} = 12 \text{ \AA}$. (b) Spectral positions of oscillations vs. $1/\bar{a}^2$.

The special treatment is needed to describe the size dependence of spectral position for excitons originating from the degenerate valence subband Γ_8 . It was shown that this dependence is given by the following expression [14]

$$\hbar\omega_{Z_{1,2}} = E_g - E_{ex} + \Delta + 0.67 \frac{\hbar^2}{2M_h \bar{a}^2} \left[\Phi(M_l/M_h) \right]^2 \quad (3)$$

where M_h and M_l are the "heavy" and "light" exciton masses, Δ is the value of spin-orbit splitting, $\Phi(M_l/M_h)$ is the root of transcendental equation [14].

Comparison between experimental and theoretical results enables us to determine the masses of exciton for all three exciton subbands: $M_s = (1.9 \pm 0.2)m_0$, $M_h = (2.6 \pm 0.2)m_0$, and $M_l = (1.5 \pm 0.2)m_0$. It is necessary to emphasize that the effective mass approximation gives the possibility to describe experimental results for the values of microcrystal radius down to about $\bar{a} \approx 15 \text{ \AA}$.

The absorption spectra of CdS microcrystals of different sizes are shown in Fig. 3a. It is seen that for the semiconductor material with a low binding energy of the exciton ($E_{ex} \approx 30 \text{ meV}$ for CdS) the decrease of microcrystal size leads to a large blue shift of the absorption band edge. Oscillations in absorption spectra of microcrystals with radius less than the exciton radius ($r_{ex} \approx 30 \text{ \AA}$) are due to quantum sublevels of conduction band [15]. As it is seen in Fig. 3b, the simple analytical expression

$$\hbar\omega_{l,n} = E_g + 0.71 \frac{\hbar^2}{2m\bar{a}^2} \Phi_{l,n}^2 \quad (4)$$

with the electron effective mass $m_e = 0.2m_0$ gives the possibility to describe the size dependence of the blue shift only for the forbidden gap width. It is clear that a nonparabolicity of the electron dispersion law and the finite depth of the quantum well have to be taken into account. The theoretical investigations of the energy spectrum of electron-hole pairs for the real band structure of the material under investigation are in progress now [16].

3. Auger-ionization of semiconductor microcrystals in glass matrix

It is well known now that optical properties of semiconductor-doped glasses are affected by photon fluency. One may observe light-induced effects of the luminescence intensity degradation (the darkening effect [3]), changes of microcrystals optical absorption spectra [17] and a decrease of the carrier life-time [18]. All of the effects are usually revealed at room temperatures but heating at 300 – 400 °C results in their disappearance.

We suggest that these effects are due to the photoionization of microcrystals in a glass matrix. The possibility of that process was demonstrated experimentally in the studies of the thermally stimulated luminescence (TSL) [17]. Figure 4a shows the TSL curves for two samples which have been illuminated at $T = 77 \text{ K}$ with light and then heated at a constant rate 0.1 K/s. The first sample was undoped and the second one was doped by CdS microcrystals with $\bar{a} \approx 30 \text{ \AA}$. The first sample was subjected to UV-light irradiation with $\hbar\omega_{ex} \approx 6 \text{ eV}$ which is in the spectral range of the interband absorption of the glass. The TSL curve for this sample

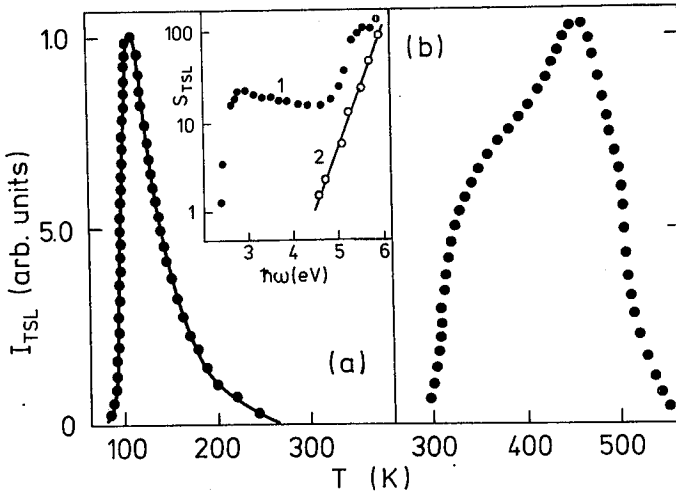


Fig. 4. Thermally stimulated luminescence curves of undoped (—) and CdS-doped glass (.....). (a) $T_{exc} = 80$ K; (b) $T_{exc} = 300$ K. Inset shows the spectral dependence of the efficiency of ionization S_{TSL} for (1) undoped glass and (2) CdS-doped glass.

which was measured within the spectral range of the intrinsic luminescence of glass is shown in Fig. 4a by a solid line. It is a typical curve which is due to the well-known electron capture centers in the glass (E_1 -centers [19]).

The second sample doped with CdS microcrystals was subjected to light irradiation from the region of the absorption edge of the microcrystals ($h\omega \approx 3.5$ eV). The TSL in this sample was registered within the spectral range corresponding to the impurity luminescence of the microcrystals. This curve is shown in Fig. 4a by points. A coincidence of these curves directly shows that nonequilibrium electrons have a finite probability to leave microcrystals and be captured by the same capture centers of glass in the vicinity of the microcrystal. Sample heating leads to going back of the electrons to microcrystals with their subsequent radiative recombination with holes. The inset in Figure 4a shows the spectral dependence of the ionization efficiency for microcrystals. It is seen that the ionization starts at the energies of the excitation quanta corresponding to the band gap of microcrystals. The increase of the efficiency at the energy of about 4.5 eV is due to the above-barrier transitions of electrons from the microcrystal into the glass.

The effect of the photoionization of microcrystals under photon flux is also observed at room temperature. Figure 4b shows the relevant TSL curve. It is seen that electrons in this case are captured by deeper traps and heating to about 600 K is needed to empty them.

We suppose that the process of the photoionization of microcrystals is accompanied by a decrease of the carrier life-time, degradation of the luminescence intensity, and other light-induced effects due to the strong enhancement of non-radiative processes in them. The mechanism of the nonradiative recombination in

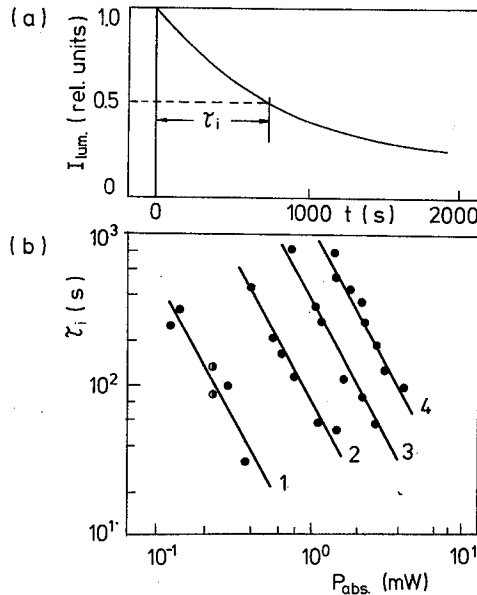


Fig.5. (a) The dependence of luminescence intensity on time of steady state excitation for CdS microcrystals with $\bar{a} = 22 \text{ \AA}$. (b) The dependence of ionization time τ_i on absorbed power for microcrystals with different sizes (1) $\bar{a} = 13 \text{ \AA}$, (2) 16 \AA , (3) 22 \AA , (4) 33 \AA .

the ionized microcrystal is beyond the scope of today's discussion. We shall discuss now the microscopic mechanism of the photoionization of microcrystals.

Figure 5a shows the dependence of the photoluminescence intensity on time of optical excitation measured on the samples with $\bar{a} = 22 \text{ \AA}$. The $\lambda = 406 \text{ nm}$ line of a krypton laser was used for the steady-state excitation. Studies were performed at the temperature of $T = 77 \text{ K}$. The kinetics of the degradation is not exponential and, to a first approximation, we shall characterize it by the time τ_i during which the intensity is diminished by a factor of 2. Figure 5b shows the degradation kinetics (in logarithmic scale) as a function of the absorbed power for the samples of different microcrystals sizes. The ionization time τ_i is seen to be strongly size-dependent and also inversely proportional to the square of the absorbed power. This observation indicates the two-photon character of the ionization process.

The qualitative model used for the analysis of the experimental results is as follows:

1. The ionization of microcrystals is the result of the Auger recombination process in the microcrystals containing two nonequilibrium electron-hole pairs. It is the many-electron process in which the energy of the electron-hole pair annihilation is transferred to the electron. If this energy is larger than the

barrier height, the electron ejects into glass and the ionization of microcrystals takes place. It is worthy to mention here that the role of the Auger processes in microcrystals at high excitation densities has been demonstrated experimentally [3].

2. The ionized microcrystals have a very low quantum efficiency of luminescence. A strong enhancement of the nonradiative channel may, for instance, be the result of an effective Auger recombination in ionized microcrystals since three quasiparticles (one electron and two holes) appear as a result of the one-photon excitation.

Thus, the luminescence intensity reflects in this case the number of yet non-ionized microcrystals. The ionization rate ($1/\tau_i$) is equal to the probability for the existence of the microcrystals with two nonequilibrium electron-hole pairs times the Auger annihilation rate

$$\tau_i^{-1} = (W_{01}\tau_0^1)(W_{02}\tau_0^2)\tau_A^{-1} \quad (5)$$

where W_{01} and W_{02} are the probabilities of photon absorption in nonexcited microcrystals and microcrystals containing one electron-hole pair; τ_0^1 and τ_0^2 are carrier life-times in the microcrystals with one and two electron-hole pairs. τ_A^{-1} is the probability of the Auger recombination in the microcrystal with two electron-hole pairs. At low intensity of excitation W_{01} and $W_{02} \sim I_{ex}$.

The calculation of the Auger recombination probability is a difficult problem because it demands the exact calculations of the small overlap integrals of the electron-hole states. Therefore, the electron-hole wave functions of the zero-dimensional quantum size structures should be considered within the many-band approximation. The second problem is that the electron ejection from the microcrystal (ionization of them) demands consideration of the quantum structure with the finite depth of the quantum well. This consideration was made within the framework of the Kane model by Al. Efros and V. Kharchenko [16]. Size dependence of the rate of the Auger ionization in microcrystals was obtained by numerical calculations for CdS ($E_g = 2.6$ eV, $m_e = 0.2m_0$) microcrystals embedded in the matrix of an oxide glass ($E_g = 7$ eV). The dependence obtained is shown in Fig. 6 by the solid line. The probability of the Auger ionization is seen to be of a pronounced oscillatory character. The maxima are related to the microcrystals where electronic quantum-size levels cross the boundary of a continuous spectrum or are situated in the neighborhood of it. In real glass samples the averaging of oscillations of $1/\tau_A$ takes place due to dispersion of microcrystal sizes and shapes, fluctuation of the microcrystal-glass band offset, etc.

We obtained the experimental values of $\tau_A(a)$ from experimental dependence $\tau_i(\bar{a})$ using Eq.5. For that it is necessary to estimate the steady state share of microcrystals containing two electron-hole pairs. Estimating that one as the square of steady state share of one excited microcrystal $W_{01}\tau_0 \approx 10^{-5}$ we obtain in our experiment that $\tau_A = (W_{01}\tau_0^1)^2\tau_i \approx 10^{-10}\tau_i$ (the value $W_{01}\tau_0^1 \approx 10^{-5}$ was estimated from the absorbed power). The probability of Auger-disintegration τ_A^{-1}

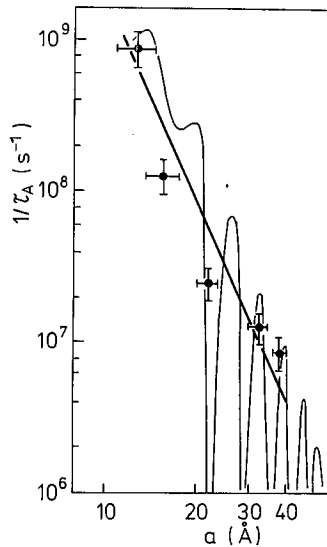


Fig.6. The theoretical dependence of the Auger ionization probability of CdS microcrystals on their radius. The crosses show the experimental data.

obtained in such a way is shown in Fig. 6 by crosses. It is seen that the experimental data are in a good agreement with theoretical dependence.

Thus the obtained results demonstrate that the ionization of microcrystals embedded in the glass matrix is due to the Auger recombination which takes place in the microcrystals containing two photoexcited electron-hole pairs at the same time. Further studies, both experimental and theoretical, have to be performed to understand the energy spectrum of the ionized microcrystals and features of relaxation and recombination processed in them.

References

- [1] A.I. Ekimov, Al.L. Efros, A.A. Onushchenko, *Solid State Commun.* **56**, 921 (1985).
- [2] D.S. Chemla, D.A.B. Miller, *J. Opt. Soc. Am. B* **2**, 1155 (1985).
- [3] P. Roussignol, D. Ricard, J. Lukasik, C. Flytzanis, *J. Opt. Soc. Am. B* **4**, 5 (1987).
- [4] A.I. Ekimov, A.P. Scvortsov, T.V. Shubina, S.K. Shumilov, Al.L. Efros, *J. Tech. Phys.* **59**, 202 (1989).
- [5] V.V. Golubkov, A.I. Ekimov, A.A. Onushchenko, V.A. Tsekhomskii, *Fiz. Khim. Stekla* **7**, 397 (1981).
- [6] T. Itoh, T. Kirihara, *J. Lumin.* **31**, 120 (1984).
- [7] R. Rossetti, S. Nakahara, L.E. Brus, *J. Chem. Phys.* **79**, 1086 (1983).

- [8] I.M. Lifshits, V.V. Slesov, *Zh. Eksp. Teor. Fiz.* **35**, 479 (1958).
- [9] N.F. Borrelli, D.W. Hall, H.J. Holland, D.W. Smith, *J. Appl. Phys.* **61**, 5399 (1987).
- [10] C.T. Dameron, R.N. Reese, R.K. Mehra et al., *Nature* **338**, 596 (1989).
- [11] S. Modes, R. Lianos, *Chem. Phys. Lett.* **153**, 351 (1988).
- [12] S. Hayashi, M. Fujii, K. Yamamoto, *Jpn. J. Appl. Phys.* **28**, L1464 (1989).
- [13] M.G. Bowendi, A.R. Kortan, M.L. Steigerwald, L.E. Brus, *J. Chem. Phys.* **91**, 7282 (1989).
- [14] A.I. Ekimov, A.A. Onushchenko, A.G. Plukhin, Al.L. Efros, *Sov. Phys.-JETP* **61**, 891 (1985).
- [15] A.I. Ekimov, A.A. Onushenko, *JETP Lett.* **40**, 1136 (1984).
- [16] Al.L. Efros, V.A. Kharchenko, M.G. Ivanov, in *Proc. of Allunion Conf. Theory of Semiconductors*, Doneck 1989, p. 36.
- [17] V.V. Grabovskis, Y.Y. Dzenis, A.I. Ekimov et al. *Sov. Phys. - Solid State* **31**, 149 (1989).
- [18] J.P. Zheng, H.S. Kwok, *Appl. Phys. Lett.* **54**, 1 (1989).
- [19] J.H. Mackey, H.L. Smith, A.I. Halperin, *J. Phys. Chem. Solids* **27**, 1759 (1966).

Quantum size effect in three-dimensional microscopic semiconductor crystals

A. I. Ekimov and A. A. Onushchenko, *JETP Lett.* **34**, 345 (1982)

http://www.jetpleters.ac.ru/ps/1517/article_23187.pdf

Interband absorption of light in a semiconductor sphere

Al. L. Efros and A. L. Efros, *Sov. Phys. Semicond.* **16**, 772 (1982)

Quantum size effect in the optical spectra of semiconductor microcrystals

A. I. Ekimov and A. A. Onushchenko, *Sov. Phys. Semicond.* **16**, 775 (1982)

Size quantization of the electron energy spectrum in a microscopic semiconductor crystal

A. I. Ekimov and A. A. Onushchenko, *JETP Lett.* **40**, 1136 (1985)

http://www.jetpleters.ac.ru/ps/1259/article_19044.pdf

Size quantization of excitons and determination of the parameters of their energy spectrum in CuCl

A. I. Ekimov, A. A. Onushchenko, A. G. Plyukhin, and Al. L. Éfros, *Sov. Phys. JETP* **61**, 891 (1985)

http://www.jetp.ac.ru/cgi-bin/dn/e_061_04_0891.pdf

Quantization of the energy spectrum of holes in the adiabatic potential of the electron

A. I. Ekimov, A. A. Onushchenko, and Al. L. Éfros, *JETP Lett.* **43**, 376 (1986)

http://jetpleters.ac.ru/ps/1404/article_21323.pdf

Optics of zero dimensional semiconductor systems

A. I. Ekimov and Al. L. Efros, *Acta Phys. Pol. A* **5**, 345 (1991)

<http://przyrbwn.icm.edu.pl/APP/PDF/79/a079z1p01.pdf>